

Review

# Issues, Challenges, and Future Perspectives of Perovskites for Energy Conversion Applications

Boucar Diouf<sup>1</sup>, Aarti Muley<sup>2,\*</sup> and Ramchandra Pode<sup>1,\*</sup> 

<sup>1</sup> Department of Information Display, Kyung Hee University, Kyunghedae-ro, Dongdaemoon-gu, Seoul 02447, Republic of Korea; diouf@khu.ac.kr

<sup>2</sup> SIES College of Arts Science & Commerce (Autonomous), Mumbai 400022, India

\* Correspondence: aartim@sies.edu.in (A.M.); rbpode@khu.ac.kr (R.P.)

**Abstract:** Perovskite solar cells are an emerging technology that exploits the self-assembly and highly tunable bandgap properties of perovskite materials. Because of their low manufacturing cost, thin films of perovskites have attracted enormous interest and witnessed great progress. The power conversion efficiency of these devices has improved from 3.8% to 25.8%, which is a significant step forward. The formulation of innovative materials with the proper replacement of lead in perovskites is essential to reduce lead toxicity. Here, we examine the difficulties encountered in the commercialization of perovskite devices, such as material and structural stability, device stability under high temperature and humidity conditions, lifetime, and manufacturing cost. This review addresses issues such as device engineering, performance stability against the harsh environment, cost-effectiveness, recombination, optical, and resistance losses, large-area solar cell module issues, material cost analysis, module cost reduction strategy, and environmental concerns, which are important for the widespread acceptance of perovskite-based solar devices. The applications and market growth prospects of perovskite cells are also studied. In summary, we believe there is a great opportunity to research high-performance, long-lived perovskites and cells for energy applications.

**Keywords:** perovskite materials; solar cells; energy conversion efficiency; issue and challenges in commercialization



**Citation:** Diouf, B.; Muley, A.; Pode, R. Issues, Challenges, and Future Perspectives of Perovskites for Energy Conversion Applications. *Energies* **2023**, *16*, 6498. <https://doi.org/10.3390/en16186498>

Academic Editors: Sungjin Jo and Elisa Artegiani

Received: 12 July 2023

Revised: 23 August 2023

Accepted: 5 September 2023

Published: 8 September 2023



**Copyright:** © 2023 by the authors. Licensee MDPI, Basel, Switzerland. This article is an open access article distributed under the terms and conditions of the Creative Commons Attribution (CC BY) license (<https://creativecommons.org/licenses/by/4.0/>).

## 1. Introduction

Energy consumption is considered an important indicator of the social progress index of development. The most abundant and widely used energy sources for power generation are fossil fuels, such as oil, natural gas, and coal. Continued use of fossil fuels has a significant impact on climate change, animal habitat degradation, and global warming [1]. Several countries facing environmental challenges have committed to reducing their greenhouse gas emissions as part of the 2015 Paris Agreement and are now focused on replacing fossil fuels with renewable energy sources [1]. In recent years, there has been discussion about the energy transition to sustainable renewable sources, which was taken forward at the COP26 conference in Glasgow, UK, in 2021 [2]. Solar and wind energy are considered the clean energy sources of the future and are readily available around the world. Undoubtedly, solar energy and solar-powered products are the most viable alternatives to fossil fuels.

Various materials are used to manufacture solar cells that convert the solar spectrum into electrical energy. However, no photovoltaic (PV) cell can convert the entire spectrum of the sun into electrical energy. Crystalline (c-Si) solar cells are the most practically demonstrated and successfully commercialized materials. According to Ballif et al., the efficiency of Si-modules marketed in 2021 ranged from 17.4% (low-grade multi-crystalline cells) to 22.7% (high-performance back-contacted cells), with an expected average of 20% for the most commonly produced solar modules. This value is well below the Shockley Queisser limit value [3,4]. In this context, organometallic perovskites are considered to be the most promising alternatives. Perovskites are widely recognized as the likely basis for

next-generation solar cells to replace silicon due to their simpler fabrication methods, lower cost, and greater flexibility [5]. Due to the lightweight and flexible nature of perovskite devices, it is certain that the demand for perovskite devices will increase in the coming years. Furthermore, these systems have significant advantages over conventional photovoltaics, such as sensitivity to the various wavelengths of the solar radiation spectrum that the panels absorb [6]. One of the most important advantages of perovskites is their high tolerance to defects in their structure. In fact, they can operate well with numerous imperfections and impurities. In recent years, hybrid perovskites have shown excellent performance [7–9], and perovskite cells have achieved conversion efficiencies of around 20% [10,11]. Recent findings indicate an exceptionally rapid improvement trend in power conversion efficiency (PCE) of perovskite cells (certified at 25.8%), particularly in tandem perovskite/CIGS (25%) and perovskite/Si tandem (monolithic) solar cells (33%) [12,13]. The rapid improvement in PCE is seen as an opportunity for the commercialization of perovskite technology. Despite increasing research and investment in perovskite-based solar cells, manufacturers must overcome certain significant obstacles to become commercially competitive. An attempt is therefore made here to address some of the difficulties faced by perovskite solar cells.

The purpose of this review article is to discuss perovskite materials in terms of energy conversion efficiency and stability. Section 2 describes the evolution of perovskite materials. Section 3 discusses the operation mechanism and development of perovskite solar cells and thin-film-based perovskite solar cells, including inorganic, hybrid, and FAMA-based perovskite solar cells. Section 4 discusses perovskite materials and their relevance to solar cell applications and the performance of the non-lead alternatives. Section 5 addresses issues and obstacles such as structural stability, device fabrication, longevity (lifespan), cost-effectiveness, recombination, optical and resistive losses, large-area solar module issues, material cost analysis, module cost reduction strategy, and environmental concerns. Perovskite cell applications and market growth prospects are also examined and discussed in Section 6. Section 7 summarizes the conclusions. We raise the concerns hindering the potential industrialization of perovskite-based solar cells related to device engineering, stability of performance under hard conditions, cost-effectiveness, containment of toxic lead compounds, and environment-related issues.

## 2. Perovskite Materials

Calcium titanate ( $\text{CaTiO}_3$ ) (a naturally occurring mineral), discovered by the Russian mineralogist Perovskite in 1839, is the origin of perovskite and perovskite-based materials [14]. Victor Goldschmidt (1926) conducted pioneering investigations into the structure of perovskites [15]. Several synthetic perovskites were then made and analyzed [16,17]. More than 40 naturally occurring minerals in the form of oxides, halides, hydroxides, arsenide, and intermetallic compounds have been identified in the perovskite supergroup [18]. Figure 1 depicts the classification of the perovskite system.

Perovskites are very versatile materials that have emerged as a rising star in the field of optoelectronics over the last decade, as seen in Figure 2 [19]. Solar cells, photodetectors, lasers, electrochemical cells, and light-emitting diodes are examples of optoelectronic devices based on perovskites. These devices have revolutionary applications in energy harvesting and conversion, imaging and sensing, X-ray detectors, display and communication, manufacturing, and medicine [19,20].

Perovskite materials exhibit a variety of characteristics. Long-range ambipolar charge transport, small exciton-binding energy, a high-value dielectric constant, a high absorption coefficient, ferroelectric properties, a tunable bandgap, and ease of manufacturing at low temperatures are among the key electrical, physical, and optical properties. Such favorable attributes of these materials have attracted immense interest in optoelectronic and PV applications [21]. Because of their high excitonic capabilities, mixed lead halide-layered perovskite materials have been investigated for use in thin-film light-emitting diodes (LEDs) and field-effect transistors (FETs).

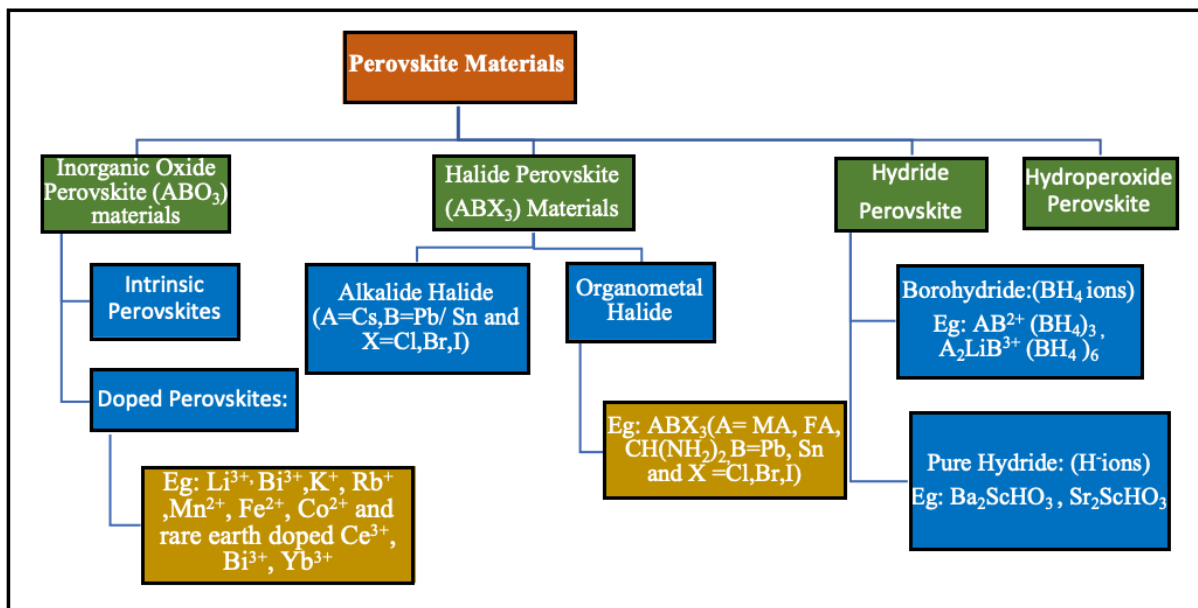


Figure 1. Classification of the Perovskite system.

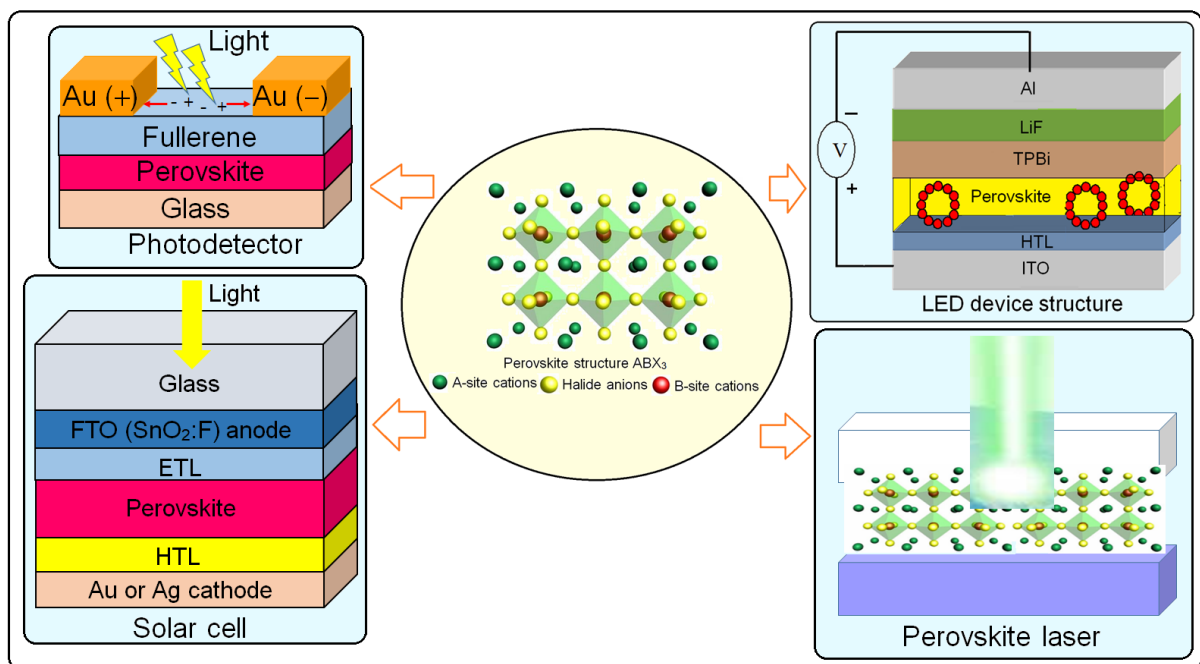


Figure 2. Optoelectronics devices based on metal halide perovskite materials and revolutionary applications.

Halide perovskites (HPs) are recognized as the most attractive and acceptable materials in PV, thermoelectric, optoelectronic radiation detection, and emission optoelectronic applications owing to their remarkable optical and excitonic properties [22–24]. Among organic halide perovskite materials, methylammonium lead triiodide (MAPbI<sub>3</sub>) is a popular organic halide perovskite material utilized in PV applications. Lead halide perovskites are the preferred material for mass production of solar panels due to their stable structure and simple and economical manufacturing procedure. Metal halide perovskites have revolutionized the solution-processable device industry and paved the way for the development of efficient flexible PV cells [25]. Ge et al. evaluated recent developments in

multidimensional metal halide perovskites for photovoltaic applications and highlighted the challenges [26].

The optoelectronic properties of hybrid metal halide perovskite materials seem promising. Zhu and Gong (2021) opined that 3D halide perovskites have unique potential for efficient optoelectronic applications [27]. The researchers also summarized the low-dimensional halide preparation procedure and addressed the systematic methodology and technical issues in 3D perovskite materials, such as inferior long-term stability, which slow down practical applications.

### 3. Operation Mechanism and Evolution of Perovskite Solar Cell

The block diagram of perovskite solar cells is shown in Figure 3a. Figure 3b depicts the operation principle of multilayer solar cells. The basic device structure contains a radiation-absorbing perovskite layer squeezed between the anode, which is commonly F-doped  $\text{SnO}_2$ , and a high-work-function cathode, such as Ag or Au metal. The light absorption by the solar cells results in the formation of excitons (a quasiparticle comprising a pair of positive (hole) and negative (electron) charges) in their absorbing layer (the perovskite material layer). The incident photons excite the electrons to a higher energy level, leaving holes behind. The charge transport layers are frequently used in devices to facilitate the movement of the accumulated charges that generate an electric current in the circuit.

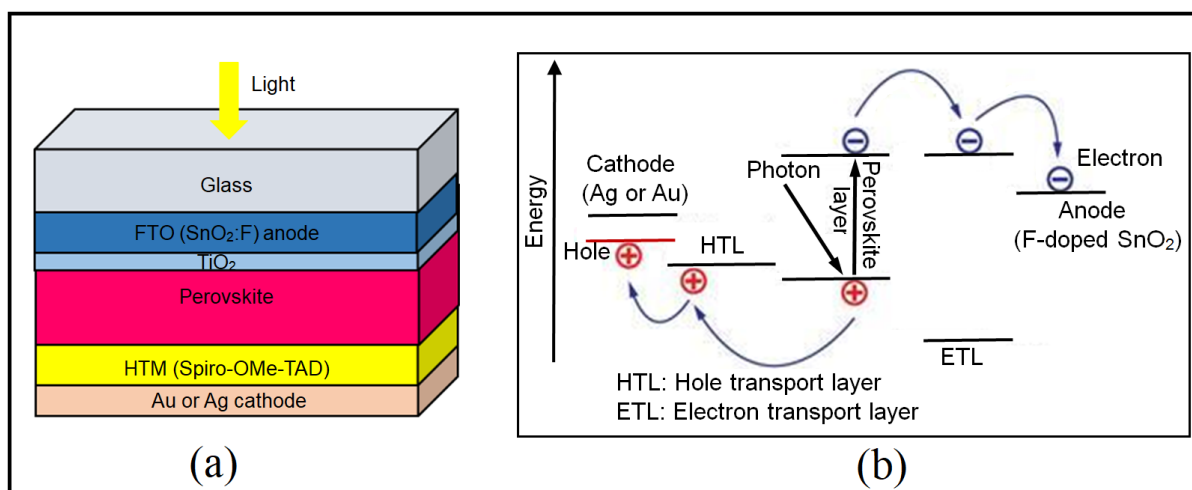


**Figure 3.** (a) Schematic diagram of perovskite solar cells. (b) Operational principle of the multilayer solar cell.

Initially, the perovskites were created on DSSC and combined with a thin perovskite layer on a mesoporous  $\text{TiO}_2$  substrate that acted as an electron collector, resulting in a PCE of 3.8% [28]. Using the same concept of DSSC, Park et al. (2011) obtained a PCE of up to 6.5% [29]. Later, using a solid-state electrolyte that behaved as a hole transport material (HTM), an efficiency of 9.7% was attained [30]. Heo et al. (2013) found that the PCE increased up to 12% using an HTM-based perovskite solar cell (PSC) with poly(triarylamine) layers [31]. The observed efficiency was further improved to 12.3% by using a mixed halide  $\text{CH}_3\text{NH}_3\text{PbI}_{3-x}\text{Br}_x$  perovskite structure [32]. The introduction of small-radius bromide (Br) ions and the phase transition from tetragonal to cubic structure, which provided stability to perovskite, were attributed to the efficiency of the mixed halide.

Later, Zang et al. (2015) improved efficiency (up to 15.2%) by introducing a pinhole-free perovskite layer utilizing a non-halide ( $\text{PbAC}_2$ ) under direct sunlight irradiation [33]. Such a substantial efficiency improvement (>15%) and stability were reported by several researchers when the devices were fabricated using  $\text{PbX}_2$  ( $X=\text{Cl}$  and  $\text{I}$ ) utilizing solution deposition and thermal evaporation techniques [34–37]. By altering the energy bands of the mixed halides [38] and modifying the thickness of the perovskite-infiltrated  $\text{TiO}_2$  frame

link to the constant perovskite layer [39], this PCE performance was improved by up to 16.2%. According to Shin et al. (2017), adjusting the band configuration of HTM/ETM (hole/electron transport material) improves the efficiency from 19.3% to 20.1% [40].

A dramatic rise in the efficiency of perovskite solar cells from 3.8% to 20% between 2009 and 2017 was achieved using solid-state thin-film design, a modified film formation technique, optimization of film thickness and morphology, interface engineering, and the use of the mixed-halide perovskites as a photon-absorbing layer in the cell structures [41].

#### *Thin-film-based perovskite solar cells*

Low-cost and scalable fabrication PSCs are of paramount importance for commercialization. It is a big challenge to significantly reduce their manufacturing costs. Therefore, next-generation PV technologies urgently need novel cost-reducing techniques. The development of appropriate film-forming techniques has met these requirements. Yulong Wang et al. in 2021 reported a systematic overview of applicable printing technologies that can potentially be used to scale up production [42]. In recent years, thin-film-based perovskite solar cells have gained popularity because of their ability to process precursors in solution form and deposit films from the solution. Various techniques, such as spin coating, blade coating, spray coating, inkjet printing, and slot-die printing, have been employed to fabricate perovskite thin-film solar cells. The low-temperature deposition of organic–inorganic perovskite thin films through simple solution processes is one of the key advantages of PSCs. In the thin-film deposition structure, the quality of the ETL and HTL interfaces with the perovskite thin film, as well as the quality of the perovskite thin film, are very important to achieve high-performance PSCs. Z. Saki et al. in 2021 explored various scalable solution-processed perovskite deposition techniques to provide a comprehensive insight into achieving high-quality, large-area perovskite thin films [43]. They also discussed the existing challenges and opportunities to promoting the commercialization of PSCs. Recently, Changshun Chen et al. showed that screen printing offers a high level of functional layer compatibility, pattern design flexibility, and large-scale capabilities, which are promising [44]. Very recently, Chinese researchers at the University of Science and Technology of China developed a new form of solar cell that not only has greater efficiency but can also be mass produced at half the cost of conventional silicon cells. The perovskite thin-film solar cell, which uses a special type of compound to absorb light, has a certified efficiency of 26.1% [13,44].

### *3.1. Inorganic Perovskite Solar Cells*

Inorganic perovskite is also referred to as the  $ABX_3$  compound, where A refers to the cations (cesium:  $Cs^+$  ions) that occupy the cubo-octahedral site and  $BX_3$  occupies the octahedral site. In this structure, B represents the cation ( $Pb^{2+}$  ions) and X represents Cl, Br, or I. Table 1 summarizes recent advances in  $CsPbX_3$  (Br, I, Cl) perovskite materials, fabrication procedures, solar cell device structure, and conversion efficiency [45–50].

In recent years, bismuth halide perovskites have received much attention because of their higher absorption coefficients, more efficient charge transfer (compared to oxide perovskites), and the thermodynamic potential required for the photocatalytic  $CO_2$  reduction reaction ( $CO_2RR$ ). In addition, these materials could become a promising alternative to the highly polluting lead halide perovskites. Despite the remarkable advantages of bismuth halide perovskites, their use has been limited because of instability issues. In a recent review, Luévano-Hipólito et al. presented solutions to obtain structures that are highly stable against oxygen, water, and light, thus promoting the formation of solar fuels with promising  $CO_2RR$  efficiencies [51]. Chen et al. discussed synthesis methods, structural diversity, photophysical properties, and current and potential applications in various currently explored optoelectronic categories of Bi-based halide perovskites in a comprehensive review [52]. Furthermore, a critical perspective on the current challenges and development prospects of Bi-based halide perovskites for versatile optoelectronic applications was presented.

**Table 1.** Developments in inorganic ABX<sub>3</sub> compounds in terms of efficiency.

S. No.	Inorganic Perovskite	Method	Solar Cell Device Structure	Efficiency (%)	Ref.
1	CsPbI <sub>3</sub> and its derivative perovskite solar cells (PSC)	Solvent controlled growth	Stable $\alpha$ -phase CsPbI <sub>3</sub> . Device structure: (ITO)/SnO <sub>2</sub> /CsPbI <sub>3</sub> /Spiro-OMeTAD/Au	15.77	[46]
2	CsPbI <sub>3</sub>	PCE-based PSC via surface termination of the perovskite film using phenyl trimethyl ammonium bromide (PTMBr)	Highly stable phase due to the use of PTMBr treated with CsPbI <sub>3</sub> . Device layers: FTO/c: TiO <sub>2</sub> /perovskite/Spiro-OMeTAD/Ag	17.06	[47]
3	CsPbI <sub>3</sub>	Formamidium (FA) iodide (FAI)-coated quantum dots	TiO <sub>2</sub> /FAI-coated CsPbI <sub>3</sub> /Spiro-OMeTAD/MoO <sub>x</sub> /Al	10.7	[45]
4	CsPbI <sub>2</sub> Br	Fabrication of ZnO/C60 bilayer electron transport layer in inverted PSC PCE	FTO/NiO <sub>x</sub> /CsPbI <sub>2</sub> Br/ZnO @C <sub>60</sub>	13.3	[48]
5	CsPbI <sub>2</sub> Br	Introduction of InCl <sub>3</sub> to enhance the efficiency of inverted PSC	Yellow stable ( $\delta$ -phase). Device structure: FTO/NiO <sub>x</sub> /perovskite/ZnO@C <sub>60</sub> /Ag using InCl <sub>3</sub> :CsPbI <sub>2</sub> Br perovskite	13.74	[49]
6	CsPbI <sub>x</sub> Br <sub>3-x</sub>	Lewis base, 6TIC-4F certified, and the most efficient inverted inorganic PSC with improved photo-stability reported to date.	Inverted layer with structure FTO/NiO <sub>x</sub> /CsPbI <sub>x</sub> Br <sub>3-x</sub> /ZnO/C60/Ag	16.1 certified 15.6	[50]

### 3.2. Hybrid Perovskite Material Solar Cells

Hybrid perovskites are emerging semiconductor materials. Affordable, solution-based semiconducting materials with potential optoelectronic characteristics are promising attributes of these materials. They are suited for use in solar cells and LEDs due to their tunable bandgap [53,54], high absorption coefficient, low excitation binding energy [55,56], and balanced mobility of the charge carriers with minimal defect formation [50,57]. Rapid advances in perovskite materials have increased the efficiency of solar cells from 3.8% to 22% in a very short period of time [29,31,39]. The extensive developments of methylammonium (MA) lead halide perovskites with respect to efficiency, as well as the testing of various HTMs, have resulted in significant advancements in thin-film optoelectronics. Table 2 describes the development of hybrid perovskite cells with PCE utilizing various HTMs [29,38,39,58–61].

**Table 2.** Progress in hybrid perovskite solar cells and power conversion efficiency.

SN	Hybrid Perovskite	HTM	Device Structure	Efficiency (%)	Ref.
1.	CH <sub>3</sub> NH <sub>3</sub> PbI <sub>3</sub>	I <sup>-</sup> /I <sup>-3</sup>	CH <sub>3</sub> NH <sub>3</sub> PbI <sub>3</sub> Quantum dots (QD)/TiO <sub>2</sub> substrate	6.5	[29]
2.	CH <sub>3</sub> NH <sub>3</sub> PbI <sub>3</sub>	CuI	TiO <sub>2</sub> /CH <sub>3</sub> NH <sub>3</sub> PbI <sub>3</sub> /spiroOMeTAD	6.0	[48]
3.	CH <sub>3</sub> NH <sub>3</sub> PbI <sub>3-x</sub> Cl <sub>x</sub>	NiO	FTO/NiO/CuSCN/CH <sub>3</sub> NH <sub>3</sub> PbI <sub>3-x</sub> Cl <sub>x</sub> /PCBM/Ag	7.3	[59]
4.	CH <sub>3</sub> NH <sub>3</sub> PbI <sub>3</sub>	CuSCN	TiO <sub>2</sub> /CH <sub>3</sub> NH <sub>3</sub> PbI <sub>3</sub> /CuSCN/Au	12.4	[60]
5.	CH <sub>3</sub> NH <sub>3</sub> PbI <sub>3-x</sub> Br <sub>x</sub>	PTAA	TiO <sub>2</sub> /CH <sub>3</sub> NH <sub>3</sub> PbI <sub>3-x</sub> Br <sub>x</sub> /DMSO/PTAA/Au	16.2	[38]
6.	CH <sub>3</sub> NH <sub>3</sub> PbI <sub>3</sub>	NiO <sub>x</sub>	ITO/NiO <sub>x</sub> /CH <sub>3</sub> NH <sub>3</sub> PbI <sub>3</sub> /PCBM/Ag	16.47	[61]
7.	CH <sub>3</sub> NH <sub>3</sub> PbI <sub>3-x</sub> Cl <sub>x</sub>	spiroOMeTAD	ITO/PEIE/TiO <sub>2</sub> CH <sub>3</sub> NH <sub>3</sub> PbI <sub>3-x</sub> Cl <sub>x</sub> /spiroOMeTAD/Au	19.32	[39]

#### *FAMA-based perovskite solar cells*

Methylammonium lead iodide (MAPbI<sub>3</sub>) perovskite has been most widely studied and used for solar cell applications. Unfortunately, the short lifespan of MAPbI<sub>3</sub> has prevented it from becoming a viable alternative to silicon solar cells. MAPbI<sub>3</sub> faces several problems, such as poor thermal stability and a wider bandgap (1.55 eV) [62]. Other disadvantages associated with MAPbI<sub>3</sub> perovskite materials are humidity sensitivity, instability under heat and light conditions, and unreliability under operating conditions [63]. The material instability of MAPbI<sub>3</sub> remains a major obstacle to widespread application because of the poorly understood degradation pathways. Haifeng Yuan et al. (2016) investigated the influence of ion migration inside the perovskite structure on the material degradation by light and electric currents in MAPbI<sub>3</sub> perovskites [64]. Their results demonstrated the critical role of ion migration in perovskite degradation and highlighted possible ways to rationally increase perovskite material stability by reducing ion migration and improving morphology and crystallinity.

In the last decade, perovskite solar cells based on formamidinium lead iodide (FAPbI<sub>3</sub>) have attracted much attention. FAPbI<sub>3</sub> perovskites are believed to have higher thermal stability and a more ideal bandgap of 1.48 eV [65]. These materials have bandgap energies suitable for use in single-junction or multi-junction solar cells and show improved stability compared to their MA-based counterparts [66]. This structure has a PCE of 25.7% [13,67]. Although FAPbI<sub>3</sub> perovskites have a preferred bandgap below 1.55 eV for solar cell applications, they suffer from operational instability [68].

In 2014, Gratzel et al. were the first to use FA/MA mixed cationic perovskites to address critical issues related to device stability and performance of perovskite solar cells, but MA was still the main ingredient [69]. N.G. Park et al. formed a thin layer of MAPbI<sub>3</sub> on FAPbI<sub>3</sub> to improve the short-circuit current density [70]. Subsequently, they showed that cesium (Cs) can stabilize the black phase of FAPbI<sub>3</sub> [71]. Furthermore, they showed that mixed devices based on Cs-MA-FA cations can achieve high efficiencies of more than 22%. Since then, an increasing number of devices using FA-based perovskites as the light-absorbing layer have been implemented and achieved higher efficiency [72,73].

Wang et al. developed novel FA<sub>0.026</sub>MA<sub>0.974</sub>PbI<sub>3-y</sub>Cl<sub>y</sub>-Cu:NiO (formamidinium methylammonium (FAMA)-perovskite-Cu:NiO) and Al<sub>2</sub>O<sub>3</sub>/Cu:NiO composites and used them to fabricate highly stable and efficient PSCs through fully ambient air processes [74]. The fabricated solar cell showed a PCE of 20.67% and long-term air-, thermal-, and photo-stability, retaining 97% of the PCE for 240 days at ambient conditions (25–30 °C, 45–55% humidity). Multi-cation perovskites based on RbCsFAMA with a narrow bandgap and high lattice stability are very promising. Impressive novel devices yield record efficiencies of 25.01% (certified 24.60%) and 23.40% (certified 22.97%) for RbCsFAMA-based PSCs with aperture areas of 0.09 cm<sup>2</sup> and 1 cm<sup>2</sup>, respectively, which shows great potential for upscaling. Earlier in 2019, Y. Wang et al. showed that the FA-MA mixed cation perovskite films (MA<sub>0.85</sub>FA<sub>0.15</sub>PbI<sub>3</sub> thin films grown using CNT-NH<sub>2</sub> and MAI additives) exhibit improved charge-carrier dynamics to facilitate charge extraction and transport and achieve a PCE of 21.05% [75,76]. A Table 3 shows the efficiencies of some FAMA-based perovskite solar cells [77–93].

**Table 3.** Efficiencies and other parameters measured in FAMA-based perovskite solar cells (under standard air-mass AM1.5 global illuminations (1000 W/m<sup>2</sup>)).

Classification	Efficiency (%)	Area (cm <sup>2</sup> )	Voc (V)	Jsc (mA/cm <sup>2</sup> )	Fill Factor (%)	Ref.
Device: FTO/TiO <sub>2</sub> (c)/TiO <sub>2</sub> (M)/(FAPbI <sub>3</sub> ) <sub>0.85</sub> (MAPbBr <sub>3</sub> ) <sub>0.15</sub> /Perovskite layer (300 nm)/PTAA/Au	17.8		1.11	22.8	70.7	[77]
FTO/NiO/FA <sub>0.85</sub> MA <sub>0.15</sub> Pb(I <sub>0.85</sub> Br <sub>0.15</sub> ) <sub>3</sub> /PCBM dripped/Ag	18.75 (certified)	1.022	1.081	21.98	78.4	[78]
MA <sub>x</sub> FA <sub>1-x</sub> SnI <sub>3</sub> perovskites	9.11		0.587	20.54	72.27	[79]
FA <sub>0.75</sub> MA <sub>0.25</sub> SnI <sub>3</sub> perovskite	9.83		0.607	23.46	69.24	[80]
FA <sub>0.75</sub> MA <sub>0.25</sub> SnI <sub>3</sub> (SnF <sub>2</sub> ) ITO/PEDOT:PSS/FA <sub>0.75</sub> MA <sub>0.25</sub> SnI <sub>3</sub> /C <sub>60</sub> /BCP/Ag	8.12		0.61	21.20	63	[81]
FA <sub>0.75</sub> MA <sub>0.25</sub> SnI <sub>2.75</sub> Br <sub>0.25</sub> (SnF <sub>2</sub> + MAI). Device: ITO/PEDOT:PSS/FA <sub>0.75</sub> MA <sub>0.25</sub> SnI <sub>2.75</sub> Br <sub>0.25</sub> /C <sub>60</sub> /BCP/Ag	8.07		0.52	22.30	70	[82]
FTO/TiO <sub>2</sub> /(FAPbI <sub>3</sub> ) <sub>0.85</sub> (MAPbBr <sub>3</sub> ) <sub>0.15</sub> /spiro-OMeTAD/Au	18.32	1	1.102	22.99	72.33	[83]
ITO/SnO <sub>2</sub> /(FAPbI <sub>3</sub> ) <sub>1-x</sub> (MAPbBr <sub>3</sub> ) <sub>x</sub> /spiro-OMeTAD/Au	20.9 (certified)	0.0737	1.116	23.9	80.6	[84]
FTO/TiO <sub>2</sub> -Cl/FA <sub>0.85</sub> MA <sub>0.15</sub> PbI <sub>2.55</sub> Br <sub>0.45</sub> /Spiro-OMeTAD/Au	19.5 (certified)	1.10	1.195	21.5	75.7	[85]
Cs <sub>0.05</sub> MA <sub>y</sub> FA <sub>0.95-y</sub> PbI <sub>3-x</sub> Cl <sub>x</sub>	20.68		1.10	24.15	78	[86]
FTO/TiO <sub>2</sub> (c)/TiO <sub>2</sub> (M)/FA <sub>0.85</sub> MA <sub>0.15</sub> Pb(I <sub>0.85</sub> Br <sub>0.15</sub> ) <sub>3</sub> /Spiro-MeOTAD/Au	19.43	0.16	1.123	22.89	75.6	[87]
FTO/TiO <sub>2</sub> (c)/TiO <sub>2</sub> (M)/(FAPbI <sub>3</sub> ) <sub>0.95</sub> (MAPbBr <sub>3</sub> ) <sub>0.05</sub> /DM*/Au	22.6 (certified)	0.0939	1.1268		80.5	[88]
FTO/TiO <sub>2</sub> (c)/TiO <sub>2</sub> (M)/(FAPbI <sub>3</sub> ) <sub>0.92</sub> (MAPbBr <sub>3</sub> ) <sub>0.08</sub> (3Dperovskite)/ <i>n</i> -hexylammonium bromide (C <sub>6</sub> Br)(LP)/Spiro-MeOTAD/Au	23.4 (22.6 certified)		1.19	24.2	78.5	[89]
Cs <sub>5</sub> (MA <sub>17</sub> FA <sub>83</sub> ) <sub>95</sub> Pb(I <sub>83</sub> Br <sub>17</sub> ) <sub>3</sub> (CsMAFA)	20.8		1.88	21.9	80.2	[90]
(FA <sub>0.65</sub> MA <sub>0.20</sub> Cs <sub>0.15</sub> )Pb(I <sub>0.8</sub> Br <sub>0.2</sub> ) <sub>3</sub>	18.19	0.06	1.15	20.06	79.8	[91]
Four-terminal tandem	(FASnI <sub>3</sub> ) <sub>0.6</sub> (MAPbI <sub>3</sub> ) <sub>0.4</sub> Cs <sub>0.05</sub> FA <sub>0.8</sub> MA <sub>0.15</sub> PbI <sub>2.55</sub> Br <sub>0.45</sub>	25.4 (certified)	0.806 1.124	10.5 20.8	80.6 79.3	[92]
All-perovskite tandem (Cs <sub>0.2</sub> FA <sub>0.8</sub> PbI <sub>1.8</sub> Br <sub>1.2</sub> /MA <sub>0.3</sub> FA <sub>0.7</sub> Pb <sub>0.5</sub> Sn <sub>0.5</sub> I <sub>3</sub> )	24.8 (certified)	20-cm <sup>2</sup>	2.157	14.86	77.5	[93]

### 3.3. Material Requirements for High Performance Solar Cell Devices

The fabrication of high-quality perovskite films with strong resistance to harsh environmental conditions and structural stability is critical for high-performance solar cell devices. Many features of perovskites have been thoroughly investigated, including direct bandgap, phase purity and stability at ambient temperature, photo-stability, and deterioration at high temperatures. Therefore, some other important features of perovskite materials that enable superior performance when compared to other semiconductors and dyes are emphasized below. These properties include the maximum absorption range, the optimal bandgap for the excitation coefficient, charge carriers' dispersion to enhance the intensity, and photoluminescence and electroluminescence emission spectra. Perovskites have a wide absorption spectrum that includes the visible and near-IR (NIR) areas. In this context, organometal halides are advantageous over dyes. With a halide film of about 600 nm thick, CH<sub>3</sub>NH<sub>3</sub>PbI<sub>3</sub> perovskite absorbs the entire visible spectrum [94]. CH<sub>3</sub>NH<sub>3</sub>PbI<sub>3</sub> has higher absorption, which is an essential requirement for any solar material. Furthermore,

the bandgap of this material is 1.55 eV. This feature, along with an extinction coefficient of  $1.5 \times 10^5 \text{ (mol/L)}^{-1} \cdot \text{cm}^{-1}$  at about 550 nm, makes  $\text{CH}_3\text{NH}_3\text{PbI}_3$  an excellent solar-radiation-absorbing material [94] and provides an exceptional quantum efficiency in the solar cell at 800 nm. Several studies have been conducted on the ambipolar behavior of  $\text{CH}_3\text{NH}_3\text{PbI}_3$  perovskite. A mesoporous  $\text{TiO}_2/\text{CH}_3\text{NH}_3\text{PbI}_3$  solar cell with a 5.5% efficiency [95] displayed a *p*-type nature. Metallic grain imperfections have been reduced in  $\text{MAPbBr}_3$ -based LEDs.  $\text{MAPbBr}_3$  nanograins are roughly 100nm thick and have an EQE of 8% [96]. With 10.8% efficiency, the mesoporous  $\text{ZnO}_2/\text{CH}_3\text{NH}_3\text{PbI}_3$  solar cell exhibits *n*-type behavior [36]. Other studies have demonstrated that  $\text{Al}_2\text{O}_3/\text{CH}_3\text{NH}_3\text{PbI}_{1-x}\text{Cl}_x$  has an *n*-type charge transport property [32,39,59,96]. The organometal halide perovskite has excellent charge carrier mobility and develops charges quickly, simplifying the manufacturing process [97]. The charge transport characteristics are primarily responsible for long-range light absorption in relation to the diffusion length of the charge carrier. The optical and electrical characteristics of methylammonium lead iodide ( $\text{MAPbX}_3$ ) perovskite are remarkable [98,99]. Absorption begins at 800nm and extends throughout the visible spectrum, with distinct free cations even at ambient temperature [100,101]. Because of the continuous tuning of the bandgap, which covers much of the visible spectrum, iodine can be a good substitute for chloride ( $\text{Cl}^-$ ) and bromide ( $\text{Br}^-$ ) [102–105]. The large bandgap value of 2.2 eV and binding energy of 150 meV of bromide in  $\text{CH}_3\text{NH}_3\text{Br}_3$ , in comparison to  $\text{CH}_3\text{NH}_3\text{I}_3$ , which has a bandgap value of 1.5 eV and binding energy of 50 meV, limit light absorption up to 550nm and thus lower the photocurrent [104] as well as the PCE [106]. Table 4 shows the classification of perovskite materials based on their properties.

**Table 4.** Classification of perovskite materials based on their characteristics.

Perovskite	Characteristics	Behavior Response
$\text{CsPbI}_3$	Bandgap	Spin-orbit coupling approximation 1.16 eV can be reduced to 0.39 eV
	Binding energy	169 eV
	Photoluminescence	$\lambda_{\text{em}} = 680 \text{ nm}$ , $\lambda_{\text{ex}} = 365 \text{ nm}$
$\text{CH}_3\text{NH}_3\text{PbBr}_3$	Absorption	800–550 nm
	Bandgap	2.2 eV
	Binding energy	150 meV
	Photoluminescence	Emission at shorter wavelength owing to larger bandgap $\lambda_{\text{em}} = 560 \text{ nm}$
$\text{CH}_3\text{NH}_3\text{PbI}_3$	Absorption	800 nm to complete visible spectrum
	The thickness of the film	600 nm
	Bandgap	1.55 eV comparable with the optimal bandgap 1.4 eV
	Binding energy	50 meV
	Photoluminescence	Emission at longer wavelength owing to small bandgap ( $\lambda_{\text{em}} = 770 \text{ nm}$ for $\lambda_{\text{ex}} = 546 \text{ nm}$ )
Ambipolar behavior	Mesoporous $\text{TiO}_2/\text{CH}_3\text{NH}_3\text{PbI}_3$	<i>p</i> -type charge transport. Solar efficiency of 5.5%
	Mesoporous $\text{ZnO}_2/\text{CH}_3\text{NH}_3\text{PbI}_3$	<i>n</i> -type charge transport. Solar efficiency of 10.8%
	Dispersion range	130 nm and 100 nm. 1100 nm and 1200 nm in $\text{CH}_3\text{NH}_3\text{PbI}_{3-x}\text{Cl}_x$

Advancements in perovskite and an increase in conversion efficiency from 3.8% to 25.8% over the decade can be credited to the frantic research and mass production of perovskite materials. Recently, highly stabilized solar cells with negligible voltage loss have been explored [89]. A perovskite device with long-term stability has displayed a PCE of approximately 25.2%. According to numerous reports, this value is close to the C-Si efficiency of 26.2%, which has dominated the market.

### 3.4. Tandem Perovskite Solar Cells

Furthermore, the PCE exceeding the Shockley–Queisser limit of single-junction solar cells could be achieved by having a tandem device configuration of perovskite and Si solar cells [107]. In tandem structures, two or more solar cells are stacked to improve the harvesting of solar energy, such as by pairing perovskite with silicon to make a tandem solar cell. Figure 4 shows the schematic structure of two-terminal and four-terminal tandem device structures. In 2015, the first perovskite/Si two-terminal tandem solar cell was reported by Mailoa et al. with an overall efficiency of 14.3% [108]. In 2016, Stanford/ASU reported the perovskite/Si tandem (monolithic) 2-terminal structure with an efficiency of 23.6, certified by NREL [13]. Later in 2018, the Oxford PV used tandem solar perovskites (perovskite/Si tandem (monolithic), 2T tandem), achieving a PCE of up to 27.3%, certified by FhG-ISE, Freiburg, Germany [13]. Silvia Mariotti of Helmholtz-Zentrum Berlin für Materialien und Energie, Germany, used an ionic liquid called piperazinium iodide to enhance their tandem solar cell (a silicon bottom cell and a perovskite top cell), achieving an efficiency rate of up to 32.5%, certified by European Solar Test Installation, Italy [109]. The record-breaking PCE of 28.6% in a perovskite-on-silicon tandem solar cell structure has been reported by Oxford PV in 2023, as independently certified by Fraunhofer ISE, Germany [110]. In addition, King Abdullah University of Science and Technology in Saudi Arabia claims they achieved 33.7 percent efficiency in a yet unpublished tandem cell test run in a new perovskite/silicon tandem solar cell, certified by the European Solar Test Installation (ESTI) [111]. LONGi, a Chinese company, announced the new conversion efficiency of 33.5% for silicon-perovskite tandem solar cells based on commercial CZ silicon wafers at the Intersolar Europe 2023 exhibition, Munich, Germany, 14 June 2023, certified by the European Solar Test Installation (ESTI) [112]. Very recently, Xin Yu Chin et al. demonstrated a certified PCE of more than 31.25% for active areas of at least 1 square centimeter in perovskite/silicon tandem cells [113].

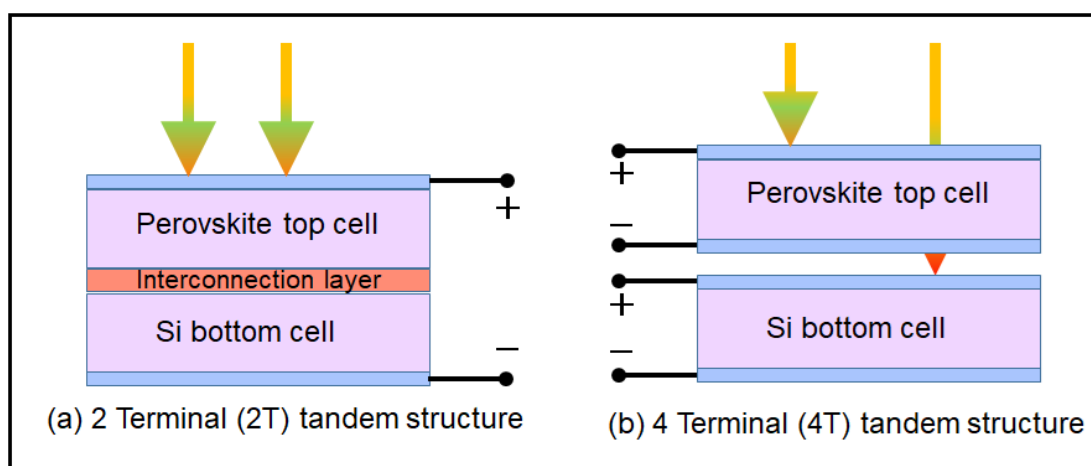


**Figure 4.** Schematic structure of two-terminal and four-terminal tandem device structures.

## 4. Perovskite Materials Concern for Solar Cell Applications

Lead-free perovskite seems to be a suitable alternative to mitigate environmental concerns. Intensive research and technological advancements in lead-based perovskites are at their pinnacle and progressing toward commercialization. The modified compounds are required to have optoelectronic properties that should be on par with Pb-based perovskites and fulfill the criteria for mass production and commercialization. Tin (Sn), bismuth (Bi), antimony (Sb), germanium (Ge), double-halide perovskite materials, and chalcogenide perovskites could become favorable compounds in perovskite solar cell applications.

#### 4.1. Sn-Based Solar Cells

Several researchers have attempted to develop Sn-based perovskites, such as  $\text{Cs}_2\text{SnA}_6$  ( $A = \text{Cl, Br, or I}$ ) [114–116] that are stable in the presence of moisture in the 4+ oxidation state. Some selected Sn-based PSCs and their properties are listed in Table 5 [117–119].

**Table 5.** Summary of selected Sn-based perovskite materials and their characteristics.

Perovskite Materials	$E_g$ (eV)	$V_{oc}$ (V)	$J_{sc}$ (mA/cm <sup>2</sup> )	FF	PCE (%)	Ref.
$\text{MASnI}_3$	1.3	0.68	16.3	0.48	5.23	[117]
$\text{MASnI}_{3-x}\text{Br}_x$	1.75	0.82	12.3	0.57	5.73	[117]
$\text{MASnIBr}_{0.8}\text{Cl}_{0.2}$	1.25	0.38	14	0.57	3	[118]
$\text{CsSnI}_{2.9}\text{Br}_{0.1}$		0.22	24.16	0.33	1.76	[119]

(where  $E_g$ —bandgap energy,  $V_{oc}$ —open-circuit voltage,  $J_{sc}$ —short-circuit current density, and FF—fill factor).

Although tin-based perovskites show great potential in PV applications, Sn-based perovskite films suffer from fast crystallization and easy formation of vacancy defects with low activation energy during the solution film-forming process, resulting in poor film quality and inferior device performance because of the high Lewis acidity and easy oxidation of  $\text{Sn}^{2+}$  [120]. The oxidation property of Sn strongly affects the device performance by creating vacancies in cells. Mohammadian-Sarcheshmeh et al. reported that the addition of uric acid in the fabrication of Sn-based perovskite solar cell causes the reduction in oxidation and carrier recombination, in turn, improves the device performance [121].

Further, a tin (Sn) perovskite is regarded as a good substitute for a lead (Pb) perovskite due to its environmental friendliness and suitable bandgap, but a Sn-based PSC suffers from practical stability and efficiency problems, which led to the introduction of the passivation material 2,5-diaminohydroquinone dihydrochloride ( $\text{C}_6\text{H}_8\text{N}_2\text{O}_2 \cdot 2\text{HCl}$ ) with  $-\text{NH}_2$  groups and  $-\text{OH}$  groups into the  $\text{FA}_{0.75}\text{MA}_{0.25}\text{SnI}_3$  perovskite [122]. This reduces the density of defect states and non-radiative recombination, suppresses the oxidation of  $\text{Sn}^{2+}$ , and reduces the neutral iodine-related defects of the aromatic structures with multiple functional groups [123].

#### 4.2. Bi-Based Solar Cells

$\text{Bi}^{2+}$  is a potential candidate for optoelectronic applications. A report on  $\text{MA}_3\text{Bi}_2\text{A}_9$  ( $A = \text{Cl, Br, or I}$ ) quantum dots, produced via synthesis using a ligand-assisted recrystallization approach, established that the tunable band can be varied from 360 to 540 nm. This wide range of variation is due to the anion composition, which gives intense emission at 423 nm with a PL quantum yield (PLQY) of around 12%. At present, a few successful results have been obtained with the Bi perovskite materials, which hold promise for replacing the Pb-based perovskites. However, some research observations have implied unfavorable results, such as a broad bandgap, low performance, and more internal defects in Bi-based perovskite materials. Some Bi-based PSCs and their properties are shown in Table 6 [124–127].

**Table 6.** Summary of selected bismuth perovskite materials and their characteristics.

Perovskite Materials	$E_g$ (eV)	$V_{oc}$ (V)	$J_{sc}$ (A/cm <sup>2</sup> )	FF	PCE (%)	Ref.
$\text{Cs}_3\text{Bi}_2\text{I}_9$	2.2	0.53	0.58	0.5	1.09	[124]
$\text{MA}_3\text{Bi}_2\text{I}_9$	2.1	0.83	3.0	0.79	3.17	[125]
$\text{MA}_3\text{Bi}_2\text{I}_9$	0.83	0.83	3.0	0.79	1.64	[126]
$\text{FA}_3\text{Bi}_2\text{I}_9$	2.19	0.48	0.11	0.46	0.022	[127]
$\text{MA}_3\text{Bi}_2\text{I}_{9-x}\text{Cl}_x$	2.4	0.04	0.18	0.38	0.003	[125]

(where  $E_g$ —bandgap energy,  $V_{oc}$ —open-circuit voltage,  $J_{sc}$ —short-circuit current density, and FF—fill factor).

#### 4.3. Sb-Based Solar Cells

Sb is a heavy metal of low toxicity that belongs to the same element group as Bi<sup>3+</sup>. Sb<sup>3+</sup> cations possess an identical electron lone pair as Pb<sup>2+</sup> and are therefore likely to replace Pb in the perovskite materials. The bandgap of inorganic Cs<sub>3</sub>Sb<sub>2</sub>I<sub>9</sub> is 2.05 eV and shows absorption comparable to that of the hybrid Pb-based perovskite CH<sub>3</sub>NH<sub>3</sub>PbI<sub>3</sub>. This material exhibits higher stability in air compared with CH<sub>3</sub>NH<sub>3</sub>PbI<sub>3</sub>. The thin films of (CH<sub>3</sub>NH<sub>3</sub>)<sub>3</sub>SbI<sub>9</sub> demonstrated a photosensitive bandgap of 2.14 eV and PL at 1.58 eV. In 2020, Ahmad and Mobin reported in a review article that the PCE of Sb-based perovskite solar cells varied from 0.03 to 3.34 [128]. Recently, antimony (Sb)-based perovskite-inspired solar cells with a PCE of 3.37 and a superior open-circuit voltage of 0.93 V have been reported by Y. Guo et al. [129]. The photovoltaic performance of some Sb-based PSCs is summarized in Table 7 [130–133].

**Table 7.** Photovoltaic performance of some Sb-based PSCs.

Perovskite Materials	E <sub>g</sub> (eV)	V <sub>oc</sub> (V)	J <sub>sc</sub> (mA/cm <sup>2</sup> )	FF	PCE (%)	Ref.
CsPb <sub>0.96</sub> Sb <sub>0.04</sub> I <sub>3</sub>		0.73	14.64	0.48	5.18	[130]
Sb-alloyed Cu <sub>2</sub> AgBiI <sub>6</sub> (Cu <sub>2</sub> AgBiI <sub>6</sub> -Sb)	1.95 eV	0.51	128	0.67	9.53	[131]
MASbI <sub>2</sub>		0.67	8.11	0.59	3.11	[132]
Cs <sub>2.4</sub> MA <sub>0.5</sub> FA <sub>0.1</sub> Sb <sub>2</sub> I <sub>8.5</sub> Cl <sub>0.5</sub>	2.0	0.6 V			6.4%	[133]

(where E<sub>g</sub>—bandgap energy, V<sub>OC</sub>—open-circuit voltage, J<sub>sc</sub>—short-circuit current density, and FF—fill factor).

#### 4.4. Ge-Based Solar Cells

Another class of materials are the Ge-based inorganic and hybrid perovskites. The experimentally measured bandgap values for CsGeI<sub>3</sub>, MAGEI<sub>3</sub>, and FAGEI<sub>3</sub> are 1.66 eV, 1.9 eV, and 2.2 eV [134], respectively. Thus, Ge materials possess desirable optoelectronic properties and could become a potential replacement for Pb in perovskite materials. Some selected Ge-based PSCs and their properties are presented in Table 8 [135–137].

**Table 8.** Summary of selected Ge-based perovskite materials and their characteristics.

Perovskite Materials	E <sub>g</sub> (eV)	V <sub>oc</sub> (V)	J <sub>sc</sub> (A/cm <sup>2</sup> )	FF	PCE (%)	Ref.
CsGeI <sub>3</sub>	1.63	0.074	5.7	0.27	1.1	[135]
MAGEI <sub>3</sub>	2.2	0.15	4.0	0.3	2.0	[136]
MAGEI <sub>2.7</sub> Br <sub>0.3</sub>		0.46	3.11	0.48	5.7	[137]

(where E<sub>g</sub>—bandgap energy, V<sub>OC</sub>—open-circuit voltage, J<sub>sc</sub>—short-circuit current density, and FF—fill factor).

#### 4.5. Double Perovskite Solar Cells

Computational investigations on the hypothetical perovskite with the general formula Cs<sub>2</sub>BB<sup>3+</sup>X<sub>6</sub> (called double perovskite) showed promising results with a bandgap in the visible region and a low effective mass [138]. McClure et al. reported the synthesis routes for the lead-free hybrid perovskites Cs<sub>2</sub>BiAgCl<sub>6</sub> and Cs<sub>2</sub>BiAgBr<sub>6</sub> [139], whereas Wei Fengxia et al. showed the synthesis of (CH<sub>3</sub>NH<sub>3</sub>)<sub>2</sub>KBiCl<sub>6</sub> double halide perovskite [140]. Lijun Zhang et al. (2017) [141] proposed the new formula A<sub>2</sub>B<sup>+</sup>B<sup>3+</sup>X<sub>6</sub><sup>VI</sup> (A = Cs<sup>+</sup>, B<sup>+</sup> = Na<sup>+</sup>, K<sup>+</sup>, Rb<sup>+</sup>) from group IA, (Cu<sup>+</sup>, Ag<sup>+</sup>, Au<sup>+</sup>) or (In<sup>+</sup>, Tl<sup>+</sup>) from group IIIB, B<sup>3+</sup> = (Bi<sup>3+</sup>, Sb<sup>3+</sup>), and X = (F<sup>-</sup>, Cl<sup>-</sup>, Br<sup>-</sup>, I<sup>-</sup>). They identified 64 such combinations and optimized them to 11 compounds with robust stability, which can be considered promising candidates for lead-free PVs. Furthermore, two compounds identified using computational methods, namely Cs<sub>2</sub>InSbCl<sub>6</sub> and Cs<sub>2</sub>InSbBr<sub>6</sub>, with bandgaps of 1.02 eV and 0.9 eV, respectively, showed theoretical solar efficiency comparable to that of CH<sub>3</sub>NH<sub>3</sub>PbI<sub>3</sub>.

#### 4.6. Chalcogenide Perovskite Solar Cells

Very recent computational simulations have proposed a new class of chalcogenide perovskites [142]. Limited studies have been presented on these perovskite materials, and some materials, such as BaZrS<sub>3</sub> [143], SrZrS<sub>3</sub> [142], BaHfS<sub>3</sub> [142], and SrHfS<sub>3</sub> [143], have been synthesized. These materials possess bandgaps and absorption coefficients that are appropriate for solar devices. Shallow point defects are observed in these materials, which provide the chance of fine-tuning charge transport and photosensitive properties. The actual experimental work is likely to open a new era in fabrication and thin-film technology and provide tailored materials for solar applications.

In summary, the merits and demerits, including challenges, of these new generations of perovskite materials, have been presented in Table 9.

**Table 9.** Summary of merits, demerits, and challenges in next-generation materials.

Materials	Merits	Demerits and Challenges
Tin (Sn) based perovskites	The optical bandgap is in the near infrared region, has a comparable ionic radius (1.35 Å) to Pb <sup>2+</sup> (1.49 Å), and exhibits stability against moisture. Sn-based materials possess stability for 3800 h. Among all lead-free materials, this material has presently achieved the highest efficiency.	Sn <sup>2+</sup> may be as hazardous as Pb <sup>2+</sup> and, therefore, may also face the same challenges that Pb-based perovskites are facing today.
Bismuth (Bi) based perovskites	Bi <sup>2+</sup> has the same electronic configuration as Pb <sup>2+</sup> (ns <sup>2</sup> ). Inorganic Bi <sup>2+</sup> -based materials show promising stability, are insoluble in water, are not toxic to the environment, are cost-effective, and have the potential to overcome most of the challenges that are faced by Pb in terms of industrialization.	Has a broad bandgap, low performance, and more internal defects. Organic compound stability is relatively low. The lowest power conversion efficiency (PCE) achieved so far in comparison with other materials Needs a more promising research direction.
	Increasing quantum yield and PCE can make this candidate an immediate replacement for Pb in the near future.	
Antimony (Sb) based perovskites	Sb <sup>3+</sup> compounds show stability in the presence of air, and the bandgap is also comparable to that of Pb (2.14 eV). They are insoluble in water, and Sb <sup>2+</sup> possesses good charge transport properties owing to the small bandgap.	(CH <sub>3</sub> NH <sub>3</sub> ) <sub>3</sub> SbI <sub>9</sub> may face the challenges of energetic disorder and low photocurrent density. low-hopping mechanism for charge transport owing to the large bandgap.
Germanium (Ge) based perovskites	These are leading materials in the semiconductor industry and possess good optoelectronic properties. Moreover, they are lightweight and less toxic to the environment. They are stable in an inert atmosphere.	Decomposes easily in the air. It is not a cost-effective material.
Double halide perovskites	Robust stability and a direct bandgap of 0.9–1.02 eV.	Most of the research is based on the computational method.

#### Performance of non-lead perovskite solar cells

Recently, Ayaydah et al. summarized most of the recent best-performing lead-free and lead-mixed Sn-based perovskite solar cells. The PCE of lead-free as well as lead-mixed TPSCs is approaching 15% and 24%, respectively [144]. They have also reported highly performing mixed Pb-Sn perovskites with Pb ≤ 50%. Xiao et al. demonstrated excellent performance of a single-junction Pb-Sn mixed PSC with a certified PCE of 20.7% [145]. Lin et al. developed a mixed Pb-Sn perovskite tandem solar cell and reported a certified efficiency of 26.4%, which exceeds that of the best-performing single-junction perovskite solar cells [146]. Encapsulated tandem devices retain more than 90% of their initial performance after 600 h of operation at the maximum power point under 1 Sun illumination in ambient conditions.

Earlier, Wang et al. presented a review in 2021 about the lead-free perovskites consisting of Sn (II), Cu (II), Bi(III), Sb (III), Sn (IV), Ti (IV), and Ag(I)Bi(III), introduced from

the isovalent and heterovalent element replacement perspectives [147]. In addition to the above-mentioned materials, the halide double perovskite has attracted people's attention because of its excellent stability and bandgap tunability. They expect that the performance and the stability of lead-free perovskites, especially 2D layered perovskites, can be continuously improved to meet the needs of commercial development.

### 5. Issues and Challenges in Perovskite Solar Cells

Substantial experimental and theoretical research has been conducted to learn about and understand the material structure, device stability, efficiency, and complex composition. In recent years, perovskite materials and technology have taken a step toward manufacturing and have explored the market for the commercialization of perovskite solar cell devices. Wang et al. opined that the mass production of PSCs is not yet feasible due to various factors [148]. Challenges faced by perovskite solar cells and modules are (i) high-quality perovskite layer fabrication with low cost and large-scale reproducibility, (ii) the choice and deposition of charge extraction layers, (iii) the fabrication of bottom and top electrodes using low-cost processes, (iv) recombination, optical, and resistance losses, and (v) lower efficiency of large cell modules. These issues need to be addressed to build small- and large-area PSC devices. In a review report, Yang et al. presented the advancement of efficient large-area PVs with stability for commercialization [149].

Furthermore, several concerns, such as lifetime, stability, lead toxicity, environmental contamination, and cost-benefit, are fundamental factors for the effective commercialization of perovskite solar cells. Perovskite compounds have great tolerance to crystalline defects because of the ionic bonding, and thin films with high crystallinity can be fabricated at low temperatures only. Further, these materials have low decomposition temperatures, making them less thermally stable than Si [150]. Recently, Lin et al. summarized the issues, such as high stability and long lifetime, lead toxicity, fabrication repeatability, large-area fabrication, and flexible devices [151]. Metal halide perovskite solar panels merits and demerits are shown in Table 10.

**Table 10.** Merits and demerits of halide perovskite solar panels.

Merits	Demerits
Hybrid perovskites with the general formula $ABX_3$ (A = organic cation, B = divalent metal, and X = halogen or pseudo-halogen) are used.	External factors, such as water, heat, humidity, and sunlight, inherently degrade the stability of the active layer of perovskite solar panels.
Easy, low-cost manufacturing processes make perovskite the obvious choice for mass production.	Water sensitivity causes irreversible damage to perovskite materials.
The PCE of perovskite solar cells is high.	Heat: Lead halides show an inability to sustain thermal stress. Therefore, the perovskite structure degrades under heat and creates halogen gases that are the source of the formation of B metals (lead, tin, germanium, etc.) on the perovskite film.
Hybrid perovskite film solar panels are confirming candidates for power generation in the near future.	Oxygen and light: Prolonged exposure to air and light photons adversely degrades the longevity of the solar panel.
Conversion energy loss is less in perovskite solar cells compared with other cells.	Scalability and efficiency on large-area perovskite are comparatively small. The technology is yet to be effectively transferred from the laboratory to industry.

Milić et al. (2021) observed that hybrid perovskites are affected by external factors such as air and moisture, photo-stability, and device operating voltage, thus resulting in various degradation routes [152]. Various strategies to overcome these instabilities, such as the use of low-dimensional hybrid perovskite materials, were proposed. Low-dimensional materials include layer-by-layer stacks of 2D perovskite and organic layers that are separated by hybrid perovskite slabs. Such a structure is more stable in ambient conditions and in ion relocation.

Although inorganic perovskites exhibit higher thermal stability, they have poorer phase stability than their hybrid counterparts. This is associated with the strain in the lattice and voids within the inorganic perovskite material crystals. In a recent review, Xiang et al. (2021) summarized and discussed the stability and lifetime mechanisms of inorganic perovskites with regard to heat, humidity, and oxygen [153]. Minimizing the vacancies and strain during the film processing may be a possible way to address the stability concerns related to both intrinsic and extrinsic factors. Challenges that need to be overcome strategically to transform perovskite modules into marketable PVs include stability, lead leakage, and outdoor testing of the modules, as discussed by Cheng et al. (2021) [154].

It may be mentioned here that lead is likely to be widely used in perovskite PV industries in the future. When the PSC panels die, the lead metal could possibly leach into the ecosystem, causing contamination of the air, earth, and groundwater. The major challenges such as material stability, device fabrication, lifetime of the devices, manufacturing cost, lead toxicity, best practices to overcome these challenges, and viable alternatives to Pb metal are discussed below.

### 5.1. Perovskite Structural Stability Perspective

The thin film of perovskites is polycrystalline and can vary with unit cell orientation. The thin-film structure of the perovskite materials is important for the stable operation of any device. A small alteration in the synthesis route and formulation can lead to a remarkable change in texture and morphology, which exert severe impacts on the device's performance. Therefore, the production of efficient and stable perovskite materials for the solar cells faces a serious challenge in defining the structure. Liu et al. (2020) examined the instability and phase behavior of FAPbI<sub>3</sub> and showed that it is highly efficient but is unstable in air and decays rapidly in a hexagonal structure [155]. Schmidt-Mende et al. (2021) [156] suggested in situ real-time scattering measurement during the film formation to obtain a better understanding of the intermediate phases formed during the process. The hybrid perovskite is expected to be highly ordered and is likely to be the best alternative for the reliable operation of devices.

### 5.2. Device Fabrication Issues

The spin-coating technique is commonly used for the deposition of a perovskite layer on the substrate in solution-processed device production. During the preparation, the solvent interacts with the precursor and forms halide complexes. The solvent plays a vital role and influences various properties of the precursor, such as its (i) solubility; (ii) evaporation rate; (iii) viscosity; (iv) crystallization; and (v) formation of the intermediate phase. The formation of several complexes occurs with the use of strong binding solvents, such as dimethyl sulfoxide (DMSO). The weak interacting solvents allow strong interaction among the starting ingredients. This leads to the creation of the intermediate phase and its subsequent conversion into the perovskite phase, which allows the rapid formation of the perovskite phase upon evaporation [157]. In contrast, strong-interacting solvents require an annealing at a higher temperature for a few minutes to obtain the pure perovskite phase [158]. The formation of these complexes can be avoided by adding a few polymer additives [159,160]. To overcome these challenges in the solution process, many reports have highlighted the step-by-step mechanism of thin-film formation.

### 5.3. Lifetime and Stability under High Temperature and Humidity

Most investigations and results reported by researchers for perovskite technology are focused on color, purity, and efficiency. However, the perovskite material and hence the stability of devices in harsh environmental conditions, such as high temperatures, weather fluctuations, and high humidity, are crucial factors to be considered seriously for commercialization. Therefore, it is vital to address the concerns of stability issues in order to simultaneously achieve high efficiency and high durability. Prolonged exposure to high

temperatures or illumination and to moisture in the air result in the degradation of the perovskites [161]. The device's performance is susceptible to oxygen, as the perovskite layers degrade when they meet oxygen [161,162]. Many researchers have argued that moisture, atmospheric oxygen, heat, etc. are possible causes of the degradation of PSCs, whereas Wang et al. (2017) stated that PSC's degradation is due to the material's natural properties [163]. Iodide-based perovskites such as MAPbI<sub>3</sub> generate a gaseous state of iodine (I<sub>2</sub>) that results in the degradation of the perovskite material. Furthermore, the acid-based chemical process used in the deposition of ZnO/MAPbI<sub>3</sub> layers causes degradation. TiO<sub>2</sub> and SnO<sub>2</sub>, used in solar cell manufacturing, demonstrate better stability, but their excessive use causes degradation when exposed to UV radiation and leads to defects [164]. The morphology of spiro-MeOTAD and additives restricts its stability. Moreover, the commonly used Au electrode atoms diffuse at high temperatures via spiro-MeOTAD, causing degradation [165]. The use of carbon electrodes is found to be highly practicable for the device's stability [166].

Compared with the hybrid organic-inorganic perovskites, all inorganic lead halide perovskites, such as CsPbI<sub>3</sub>, exhibited better thermal stability and, hence, attracted the attention of several researchers. However, their low structural stability (phase stability) under ambient conditions limits their practical applications [167]. To improve longevity, the formation of 2D and 3D perovskites was suggested as a possible alternative. Next, the long-term stability of PSCs under ambient conditions can be augmented by using proper encapsulation to protect the device from environmental changes [163,168]. Recently, Ling Xiang et al. investigated the detailed requirements for the encapsulation process and encapsulant materials to meet external challenges such as temperature, oxygen, moisture, and UV light [169]. Figure 5 shows the schematic of the encapsulation of commercial silicon and perovskite solar cells. Ethylene-vinyl-acetate (EVA) is the most commonly used encapsulation material for commercial use owing to its low cost, adequate transparency, and flexibility. However, it is prone to acetic acid formation and has a high water vapor transmission rate. Two alternatives for EVA are thermoplastic polyolefin (TPO) and polyvinyl butyral (PVB) [170]. More recently, interest in polyolefin elastomer-based (POE) and thermoplastic polyurethane (TPU) has increased. A variety of encapsulation materials, such as fluoropolymeric coatings, TPU, ethylene methyl acrylate, cyclized perfluoro-polymer (Cytop), organic-inorganic hybrid materials (ORMOCERs), ORMOSIL aero-gel thin film, and various polymer films, have been reported for perovskite solar cells [171]. Although the encapsulation method has been successfully implemented using a glass cover and inert epoxy resin, it influences the performance of the device [172,173]. Therefore, optimization of sealing is necessary to have good performance under heat and pressure stresses. Earlier, Yaoguang Rong et al. reported that the methacrylate glue, krypton polymer layer encapsulation, etc., exhibit the stable performance of the devices for more than 1300 h in dark conditions [172]. This type of encapsulation has been adopted by several researchers to achieve a significantly higher device operation lifetime. The performance of MAPbI<sub>3</sub> perovskite solar cells under various atmospheric conditions is described in Table 11 [38,174–178].

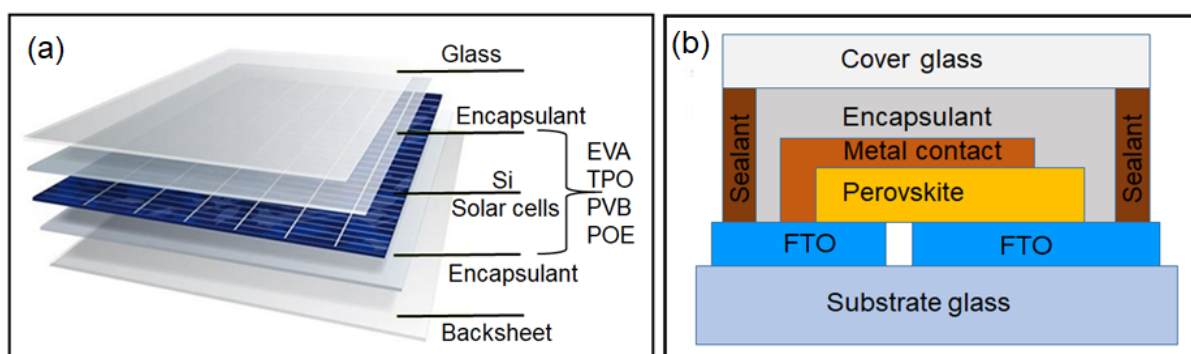


**Figure 5.** Encapsulation of solar cells: (a) commercial Si solar cells, (b) perovskite solar cells.

**Table 11.** Stability and performance of MAPbI<sub>3</sub> perovskite solar cells in response to illumination, atmospheric conditions, and encapsulation.

Solar Cell Structure	Testing Conditions						Ref.
	Stability Time (hours)	Illumination Dark/Light	Temperature (°C)	Atmospheric Condition Humidity (%)	Encapsulation	Percentage of Initial Performance (%)	
m-TiO <sub>2</sub> /MAPbI <sub>3</sub> /Carbon	>2000	Dark	RT	Air	No	100	[175]
m-TiO <sub>2</sub> /MAPbI <sub>3</sub> /PDPPDBTE/Au	1000	Dark	RT	Air (20)	No	100	[176]
ITO/NiOx/MAPbI <sub>3</sub> /ZnO/Al	1440	Dark	25	Air (30–35)	No	90	[177]
ITO/PETOD:PSS/MAPbI <sub>3</sub> /ZnO/Ag	1000	Dark	30	Air (65)	Yes	>95	[177]
m-TiO <sub>2</sub> /ZrO <sub>2</sub> /MAPbI <sub>3</sub> /Carbon	>3000	Dark	RT	Air (35)	no	~100	[174]
m-TiO <sub>2</sub> /MAPbI <sub>3</sub> /Carbon	1002	Ultraviolet	40	Air (45)	Yes	~100	[178]
BaSnO <sub>3</sub> /MaPbI <sub>3</sub> /NiO/Au	1000	Light	RT	Air	Yes	93	[38]

(Light: subjected to continuous solar illumination; Dark: storage without illumination).

#### 5.4. Alternatives to the Toxic Heavy Metal Lead

Among all perovskite materials, MAPbI<sub>3</sub> has a stable perovskite phase in air. Therefore, many researchers have focused on the optimization of this material [179,180]. However, lead in perovskite solar cells poses serious risks to human health and the ecosystem. Ren et al. (2021) examined the latest developments related to the safety issue of lead perovskite PVs and the corresponding solutions [181]. When the perovskite solar cells decay or are damaged, the released or leaked PbI<sub>2</sub> pollutes the environment, which is harmful to the human respiratory and brain systems and promotes oxidative stress [182]. Lead contamination is largely minimized in many developed countries, but the threat continues in developing countries. Nevertheless, the use of Pb in PV solar cells is likely to continue as the solar panels are pardoned from the European Legislation Restriction of Hazardous Substances [7]. The power conversion efficiency and stability of PCS cells are far better than those of lead-free PSCs. As a result, Chun-Hao Chen et al. in 2023 proposed the methodology of reducing lead leakage based on polymer resin protective layers and self-healing encapsulation, which can increase lead capture rates up to 95% under harsh conditions [183]. Since complete elimination of Pb from commercially competitive PSCs requires a considerable amount of time and resources, strategies for risk management of available Pb-based PSCs, essential for the commercialization of sustainable and environmentally viable PSCs, are reported by Kim et al. [184]. Technologies to improve the public's acceptance of the available Pb-based PSCs, such as reducing Pb leakage and a Pb-chelating encapsulation approach, were discussed in the review.

In summary, the development of Pb-free perovskite materials that are more competent, economical, and long-lasting may be the better option and is necessary.

##### Future perovskite materials—Machine learning approach

Recently, the use of computational methods and artificial intelligence (AI), referred to as machine learning (ML), has attracted worldwide attention for the prediction and assessment of perovskite materials [185]. ML is a statistical model that requires a systematic approach to data analysis based on historical data, mathematical calculations, statistics, and computer and engineering knowledge. To maintain the stability of the hybrid perovskite MAPbI<sub>3</sub>, Hartono et al. (2020) developed 21 different capping layers using the ML approach [186]. Photocurrent extraction by solar cells depends on their mobility, lifetime diffusion length, and charge carriers. Consequently, researchers examined the problem via an AI approach. They proposed that this process not only facilitated the fast screening and completed the calculations of charge carrier mobilities but also provided a straightforward path to determine the charge carrier masses, electron–phonon coupling, and phonon frequency in metal halide perovskites [187].

Currently, ML and AI techniques are widely used to understand the bandgap, stability, crystal formation, and charge carrier mobilities of perovskites. These studies are limited to small structures and differ considerably from realistic conditions, such as temperature dependence, atmospheric moisture that affects the bandgap, effective masses, thermal disorders, and structural changes [188,189]. The theoretical calculations demand a highly precise explanation of metal halide perovskites in spin-orbit coupling, interactions of charge carriers, structural properties, lattice vibrations, and the complexity of the bandgaps of hybrid and inorganic perovskite materials.

##### *5.5. Recombination, Optical, and Resistance Losses*

Although perovskite solar cells have a high PCE of up to 25.8%, they are still far from the theoretical Shockley–Queisser limit efficiency (30.5%) [4,13]. Future device performance enhancements are hampered by substantial charge recombination at the interface of the perovskite film and charge transport layers. Therefore, any further improvement in photovoltaic performance now requires a better understanding of the elementary physical processes governing energy conversion, such as charge carrier generation, transport, and recombination dynamics. To create high-efficiency perovskite cells, many strategies, such as additive engineering, defect passivation, interface engineering, and transmission material optimization, have been proposed. Chen and Park showed that trap-assisted nonradiative recombination, called Shockley–Read–Hall (SRH), in perovskite films and interface recombination are primarily responsible for the perovskite cell efficiency [190]. Suppressing bulk SRH and interface recombination improves cell efficiency. Kiermasch et al. found that the post-annealing treatment of the cell increased charge carrier lifetime, indicating a reduction in traps or their capture cross-section [191]. They also demonstrated that controlling the substrate temperature during manufacturing can reduce recombination losses.

Zhang et al. discussed the important methods for improving PCE [192]. Some of these are passivation of interface defects to reduce charge accumulation, optimization of transmission material, preparation of high-quality films, suppression of nonradiative carrier recombination and hysteresis elimination, selection of appropriate ETL and HTL materials to eliminate optical and electrical losses by effectively transferring the photo-generated charge, and interface modification to modify the energy level arrangement and the film surface morphology. Cheng et al. recently hypothesized that self-assembled monolayers for interfacial modification can improve perovskite cell performance for practical applications, realizing cost-effective and stable processing [193]. Wang et al. examined the loss factors limiting perovskite solar cell performance and concluded that SRH recombination and series resistance are the two most critical variables limiting perovskite solar cell performance [194]. They also showed that the perovskite solar cell's efficiency suffers significantly from surface recombination. Shunt resistance and surface recombination play slight roles in PCE. To approach the ultimate efficiency limit of perovskite solar cells, technologies with very high SRH lifetime and very low series resistance are necessary. Recently, Du, B. et al. reported that the deep-level traps caused by specific charged defects are the main non-radiative recombination centers, which is also the most important factor in limiting the PCE of perovskite devices [195]. The selection of appropriate passivation materials and passivation strategies to effectively eliminate defects or passivate deep defect-induced traps in perovskite films helps improve their photovoltaic performance and stability.

##### *5.6. Issues with Large-Area Solar Modules*

In the case of perovskite solar modules, upscaling has resulted in significant efficiency losses due to the difficulty of deposition of individual solar cell layers over the large surface area, and secondly, when connected in series, so-called dead areas arise between the active solar cell strips. As the dead areas are necessary for series connection but do not contribute to the generation of electricity, the focus should be on optimizing the actual solar cell layer stack as well as further reducing the size of the dead zones. Single-cell interconnections also cause fill factor (FF) degradation during upscaling processes. This degradation has been

attributed to the resistance of the transparent conducting oxide (TCO), unremoved layers even after scribing processes, and damage during scribing processes. Furthermore, the difficulties associated with large-area perovskite solar cells originate from the limitations of the thin-film solar module design. The conventional spin-coating process has limitations when used for large-area deposition processes. The nonuniformity of materials can cause drops in the open-circuit voltage ( $V_{OC}$ ). Sang-Won Lee et al. investigated the state and issues of upscaling research on perovskite solar cells in 2020, which must be addressed for commercialization efforts to succeed [196]. They reported an  $804\text{ cm}^2$  perovskite solar module with 17.9% efficiency, which is significantly lower than the 25.2% efficiency of a  $0.09\text{ cm}^2$  perovskite solar cell.

### 5.7. Manufacturing Cost

The affordability of any electronic device relies on its performance and long lifespan. The cost–performance ratio is calculated based on the expenses incurred regarding the raw materials used, fabrication of the device, labor, operation, overhead cost, and disposal or recycling. These factors together constitute the capital cost, which must be taken into consideration during the commercialization of the product. Although no standard lifetime has been reported for perovskites, it is assumed to be  $>1000\text{ h}$  and needs to be further improved. Other constituents that added to the cost were the back-contact electrodes made of gold or silver. These are costly metals, and it is hence necessary to develop economical contact materials. Alternatively, the use of highly stable carbon electrodes may reduce expenses and improve stability [175]. Copper electrodes could also be considered as an alternative in high-performance solar perovskites [197]. In addition to these issues, the main concern is the presence of lead halide in the perovskites. To minimize lead toxicity in the environment, recycling and reuse of lead (Pb) are recommended. However, recycling is economical only when there is a large active market [198,199]. Furthermore, the conductive glass (FTO) used in solar cells is the most expensive part, which can be reused without reducing the performance of the devices.

#### 5.7.1. Material Cost Analysis

Perovskite cell technology promises a cheaper alternative to the most widely accepted photovoltaic technology, with lower production costs, material costs, and energy demands during the manufacturing process. In order to be competitive with crystalline Si, the overall cost of perovskite cells must be reduced. The material costs include front glass and processing, active layers, back sheet, encapsulation and stringing, and junction box costs. The careful selection of the materials could make the formulation of the perovskite active layer practical for commercial-scale production. According to Vidal et al., the current production costs of perovskite cells could be reduced if a decrease in or suitable alternative low-cost barrier foils and transparent conductive oxide-coated plastics could be found [200]. Changes in raw material pricing may pose a challenge to the perovskite solar energy market. Sofia et al. presented a techno-economic analysis of perovskite-silicon tandem solar modules in 2020, and explored the cost-performance for silicon bottom cells in perovskite-silicon tandems [201]. They demonstrated that by utilizing current, low-cost multi-crystalline silicon technology, perovskite-silicon tandems can become cost-effective and competitive, and provide adequate advantages for investment.

#### 5.7.2. Panel Cost Analysis

Researchers from Australia and the United States presented a method for calculating the manufacturing costs of perovskite photovoltaic modules, which are estimated to cost  $107\text{ US}/\text{m}^2$  (uncertainty range  $87$  to  $140\text{ US}/\text{m}^2$ ) [202]. The estimated cost is comparable to the costs of commercial crystalline silicon and cadmium telluride photovoltaic technologies. Chang et al. argued in 2018 that because the perovskite module is still in its early stages of development and much of the device research is focused on the solar cell scale, it is difficult to estimate these costs accurately [203]. According to Mark Hutchins' recent

report, the scientists devised new measurements that projected the production of 100 MW of perovskite solar cells [204]. The report also claims that there are numerous possible commercialization options for the product. Pavel Čulík et al. recently demonstrated that the production of perovskite solar panels necessitates a process cost calculation model that takes into account variable climate conditions and labor costs at various installation locations [205]. They showed that perovskite PV production is competitive with standard Si PV technologies, even at lower production scales.

### 5.7.3. Module Cost Reduction Strategy

Apart from efficiency, the cost of a photovoltaic technology also attracts attention. Providing affordable solar energy could significantly improve living conditions. It is also the main target of the U.S. Department of Energy SUNSHOT Initiative, which aims at bringing down the cost of solar electricity below 0.06 USD per kilowatt-hour over its lifetime [206]. Success with this challenge could be achieved by providing affordable PV modules. Zongqi Li et al. investigated four solar modules, namely silicon solar cells, perovskite solar cells, perovskite/silicon tandem solar cells, and perovskite/perovskite tandem solar cells, with a focus on their LCOE (levelized cost of electricity) [207]. They proposed that the tandem structures have great commercial potential if their performance (PCE and lifetime) at a laboratory scale can be achieved after scaling up with low-cost materials and with a satisfactory material utilization ratio. Recently, researchers predicted that perovskite solar cells (PSCs) are likely to have a relatively low production cost per panel and even a low LCOE compared to single-junction (S-J) silicon solar cells [205,207]. The LCOE of perovskite PV was estimated to be 3.5–4.9 US cents/kWh with a 15-year lifetime, which was even lower than that of traditional fossil energy. However, more attention should be given to improving device efficiency and lifetime rather than low-cost material replacement. Actually, perovskite cell modules are still far from suitable for practical use, and the expected device performance has not been fully achieved yet. More work is needed to enhance the efficiency and lifetime of perovskite modules, which will ultimately boost perovskite PVs' competitiveness throughout the whole energy sector. Apart from being highly efficient, the perovskite solar system is relatively more affordable than any other photovoltaic system.

## 6. Potential Applications and Market

Perovskite solar cell products are classified into two types: rigid perovskite solar cells and flexible perovskite solar cells. Because of their flexibility and light weight, these cells have applications in residential, commercial, industrial, automotive, defense, and other sectors. The end users of perovskite solar cells include aerospace, industrial automation, consumer electronics, energy, and others. The perovskite solar cells market comprises solar panels, smart glass windows, perovskite in tandem solar cells, utilities, portable devices, building-integrated photovoltaics (BIPV), and other products. According to the Precedence Research report, the global perovskite solar cell market is predicted to reach roughly US\$ 9.91 billion by 2032, with a 32% compound annual growth rate (CAGR) from 2023 to 2032 [208]. The perovskite solar cell market would grow from US\$ 120.29 million in 2023 to US\$ 2759.16 million by 2030, at a CAGR of 56.5% over the forecast period, as projected by Fortune Business Insight [209]. The key drivers of market growth include high power conversion efficiency, low manufacturing costs, and simple fabrication techniques. However, high production costs are expected to hinder the expansion of the perovskite solar sector.

## 7. Conclusions

We analyzed the challenges encountered in the commercialization of perovskite devices, such as material and structural stability, device stability under high temperatures and humidity, lifetime, and manufacturing cost. Because of their advantages, such as low cost, simple fabrication techniques, and excellent crystallinity, perovskite materials are very

practical and competitive for fabrication. Hybrid perovskites, in particular, have numerous advantages, including a high absorption coefficient, balanced charge carrier mobility, and low defect formation. As the power conversion efficiency and stability of PCS cells are far better than those of lead-free PSCs, the use of Pb in PV solar cells is likely to continue in the future. However, the toxicity and environmental issues related to Pb in perovskite materials are serious concerns that must be addressed urgently before the large-scale adoption of perovskite solar panels. To prevent mitigation of the environment and harm to human health, the proposed options are to increase the material stability, have a long lifetime of the device, employ hermetic encapsulation, have a proper disposal option, and recycle dead devices. Nonetheless, in practical applications, the deterioration of perovskite solar cells owing to prolonged exposure to high temperatures and relative humidity cannot be avoided.

Indeed, the complete removal of Pb metal from the perovskite by new non-toxic materials that possess properties like those of lead-based perovskites is necessary. Prolonged exposure to Pb may be hazardous to human health and may cause irritation to the skin, lungs, and eyes. Continuous exposure can result in serious health issues. Many elements, such as Sn, Ge, Sb, and Bi, have been proposed to replace Pb in perovskites to avoid damage to the environment. Further, the cost analysis reveals that material selection, production, and ground installation greatly reduce the cost. According to the energy payback time, the perovskite layer consumes only 1% of the input energy, whereas the manufacturing process consumes 5.3%. The sensitivity measurements show the major cost concerns are production, maintenance, and local labor. Here, we suggest that solar panels be installed on a 365-day site with hot and dry weather conditions, with local maintenance and labor, such as cleaning the panel using a robot machine.

Furthermore, ML and AI techniques are anticipated to be used to synthesize future perovskite materials with precise knowledge about their characteristics. Compounds identified by computational approaches, such as double-halide perovskites and chalcogenide perovskites, have a long way to go before dominating the market because they must go through the necessary synthesis pathway, and achieve thin-film deposition, device engineering, and thermodynamic stability. Computational research has suggested that double-halide perovskites and chalcogenide compounds could be suitable substitutes for the Pb metal.

Overall, perovskite solar cells have great potential for producing efficient and low-cost solar energy. We believe that their instability and the presence of toxic materials, along with other issues, are major market restraints. The development of solar cells that are cost-effective, efficient, and stable is necessary so that they can be widespread and accessible to the general population. In conclusion, it is indicated that the successful replacement of Pb metal, environmental concerns, cost-effectiveness, and industrialization issues must be addressed in order for perovskite solar cells to be widely accepted.

**Author Contributions:** Conceptualization, A.M. and R.P.; methodology, A.M. and R.P.; formal analysis, B.D.; investigation, A.M. and R.P.; writing—original draft preparation, A.M. and R.P.; writing—review and editing, B.D.; supervision, R.P. All authors have read and agreed to the published version of the manuscript.

**Funding:** This research received no external funding.

**Data Availability Statement:** Not applicable.

**Conflicts of Interest:** The authors declare no conflict of interest.

## References

1. Nunez, C. Learn How Human Use of Fossil Fuel Non-Renewable Energy Resources Coal, Oil, and Natural Gas-Affect Climate Change. *National Geographic*. 2 April 2019. Available online: <https://www.nationalgeographic.com/environment/article/fossil-fuels> (accessed on 25 November 2021).
2. United Nations Climate Change Conference, Glasgow, UK from 31 October–13 November 2021. Available online: <https://earth5r.org/cop26-the-negotiations-explained/> (accessed on 1 January 2022).

3. Ballif, C.; Haug, F.J.; Boccard, M.; Verlinden, P.J.; Hahn, G. Status and perspectives of crystalline silicon photovoltaics in research and industry. *Nat. Rev. Mater.* **2022**, *7*, 597–616. [CrossRef]
4. Shockley, W.; Queisser, H.J. Detailed balance limit of efficiency of p-n junction solar cells. *J. Appl. Phys.* **1961**, *32*, 510–519. [CrossRef]
5. MIT News. Explained: Why Perovskites Could Take Solar Cells to New Heights. Available online: <https://news.mit.edu/2022/perovskites-solar-cells-explained-0715> (accessed on 1 July 2023).
6. Akihiro, K.; Teshima, K.; Shirai, Y.; Miyasaka, T. Organometal halide perovskites as visible-light sensitizers for photovoltaic cells. *J. Am. Chem. Soc.* **2009**, *131*, 6050–6051.
7. Green, M.A.; Ho-Baillie, A.; Snaith, H.J. The emergence of perovskite solar cells. *Nat. Photonics* **2014**, *8*, 506–514. [CrossRef]
8. Snaith, H.J. Perovskites: The emergence of a new era for low-cost, high-efficiency solar cells. *J. Phys. Chem. Lett.* **2013**, *4*, 3623–3630. [CrossRef]
9. Park, N.-G. Perovskite solar cells: An emerging photovoltaic technology. *Mater. Today* **2015**, *18*, 65–72. [CrossRef]
10. Julian, B.; Pellet, N.; Moon, S.-J.; Humphry-Baker, R.; Gao, P.; Nazeeruddin, M.K.; Grätzel, M. Sequential deposition as a route to high-performance perovskite-sensitized solar cells. *Nature* **2013**, *499*, 316–319.
11. Zhang, W.; Anaya, M.; Lozano, G.; Calvo, M.E.; Johnston, M.B.; Míguez, H.; Snaith, H.J. Highly efficient perovskite solar cells with tunable structural color. *Nano Lett.* **2015**, *15*, 1698–1702. [CrossRef]
12. Wang, R.; Huang, T.; Xue, J.; Tong, J.; Zhu, K.; Yang, Y. Prospects for metal halide perovskite-based tandem solar cells. *Nat. Photonics* **2021**, *15*, 411–425. [CrossRef]
13. National Renewable Energy Laboratory. Best Research-Cell Efficiencies. Available online: <https://www.nrel.gov/pv/assets/pdfs/best-research-cell-efficiencies.20200925.pdf> (accessed on 1 July 2023).
14. Katz, E.A. Perovskite: Name puzzle and German-Russian odyssey of discovery. *Helv. Chim. Acta* **2020**, *103*, e2000061. [CrossRef]
15. Goldschmidt, V.M. Die gesetze der krystallochemie. *Naturwissenschaften* **1926**, *14*, 477–485. [CrossRef]
16. Halasyamani, P.S. Noncentrosymmetric Inorganic Oxide Materials: Synthetic Strategies and Characterization Techniques. In *Functional Oxides*; O'Hare, D., Walton, R.I., Bruce, D.W., Eds.; John Wiley & Sons, Ltd.: Hoboken, NJ, USA, 2010; pp. 1–40, ISBN 9780470997505.
17. Goel, P.; Sundriyal, S.; Shrivastav, V.; Mishra, S.; Dubal, D.P.; Kim, K.-H.; Deep, A. Perovskite materials as superior and powerful platforms for energy conversion and storage applications. *Nano Energy* **2021**, *80*, 105552. [CrossRef]
18. Locock, A.J.; Mitchell, R.H. Perovskite classification: An Excel spreadsheet to determine and depict end-member proportions for the perovskite-and vapnikite-subgroups of the perovskite supergroup. *Comput. Geosci.* **2018**, *113*, 106–114. [CrossRef]
19. Dong, H.; Ran, C.; Gao, W.; Li, M.; Xia, Y.; Huang, W. Metal Halide Perovskite for next-generation optoelectronics: Progresses and prospects. *eLight* **2023**, *3*, 3. [CrossRef]
20. Baeva, M.; Gets, D.; Polushkin, A.; Vorobyov, A.; Goltaev, A.; Neplokh, V.; Mozharov, A.; Krasnikov, D.V.; Nasibulin, A.G.; Mukhin, I.; et al. ITO-free silicon-integrated perovskite electrochemical cell for light-emission and light-detection. *Opto-Electron. Adv.* **2023**, *6*, 220154. [CrossRef]
21. Thomas, S.; Thankappan, A. (Eds.) *Perovskite Photovoltaics: Basic to Advanced Concepts and Implementation*; Academic Press: Cambridge, MA, USA, 2018; pp. 197–229.
22. Orrea-Baena, J.-P.; Saliba, M.; Buonassisi, T.; Grätzel, M.; Abate, A.; Tress, W.; Hagfeldt, A. Promises and challenges of perovskite solar cells. *Science* **2017**, *358*, 739–744. [CrossRef] [PubMed]
23. Lin, K.; Xing, J.; Quan, L.N.; García de Arquer, F.P.; Gong, X.; Lu, J.; Xie, L.; Zhao, W.; Zhang, D.; Yan, C.; et al. Perovskite light-emitting diodes with external quantum efficiency exceeding 20 per cent. *Nature* **2018**, *562*, 245–248. [CrossRef]
24. Akkerman, Q.A.; Manna, L. What defines a halide perovskite? *ACS Energy Lett.* **2020**, *5*, 604–610. [CrossRef]
25. Hoefler, S.F.; Trimmel, G.; Rath, T. Progress on lead-free metal halide perovskites for photovoltaic applications: A review. *Monatshefte Für Chem. Chem. Mon.* **2017**, *148*, 795–826. [CrossRef]
26. Ge, C.; Xue, Y.Z.B.; Li, L.; Tang, B.; Hu, H. Recent Progress in 2D/3D Multidimensional Metal Halide Perovskites Solar Cells. *Front. Mater.* **2020**, *7*, 601179. [CrossRef]
27. Zhu, T.; Gong, X. Low-dimensional perovskite materials and their optoelectronics. *InfoMat* **2021**, *3*, 1039–1069. [CrossRef]
28. Green, M.A. Silicon solar cells: Evolution, high-efficiency design and efficiency enhancements. *Semicond. Sci. Technol.* **1993**, *8*, 1. [CrossRef]
29. Im, J.-H.; Lee, C.-R.; Lee, J.-W.; Park, S.-W.; Park, N.-G. 6.5% efficient perovskite quantum-dot-sensitized solar cell. *Nanoscale* **2011**, *3*, 4088–4093. [CrossRef]
30. Kim, H.-S.; Lee, C.-R.; Im, J.-H.; Lee, K.-B.; Moehl, T.; Marchioro, A.; Moon, S.-J.; Humphry-Baker, R.; Yum, J.-H.; Moser, J.E.; et al. Lead iodide perovskite sensitized all-solid-state submicron thin film mesoscopic solar cell with efficiency exceeding 9%. *Sci. Rep.* **2012**, *2*, 591. [CrossRef] [PubMed]
31. Heo, J.-H.; Im, S.-H.; Noh, J.-H.; Mandal, T.N.; Lim, C.-S.; Chang, J.-A.; Lee, Y.-H.; Kim, H.-S.; Sarkar, A.; Nazeeruddin, M.K.; et al. Efficient inorganic–organic hybrid heterojunction solar cells containing perovskite compound and polymeric hole conductors. *Nat. Photonics* **2013**, *7*, 486–491. [CrossRef]
32. Noh, J.-H.; Im, S.-H.; Heo, J.-H.; Mandal, T.N.; Seok, S.-I. Chemical management for colorful, efficient, and stable inorganic–organic hybrid nanostructured solar cells. *Nano Lett.* **2013**, *13*, 1764–1769. [CrossRef]

33. Zhang, W.; Saliba, M.; Moore, D.T.; Pathak, S.K.; Hörantner, M.T.; Stergiopoulos, T.; Stranks, S.D.; Eperon, G.E.; Alexander-Webber, J.A.; Abate, A.; et al. Ultrasoft organic–inorganic perovskite thin-film formation and crystallization for efficient planar heterojunction solar cells. *Nat. Commun.* **2015**, *6*, 6142. [[CrossRef](#)] [[PubMed](#)]
34. Chang, Y.H.; Park, C.-H.; Matsuishi, K. First-principles study of the Structural and the electronic properties of the Lead-Halide-based inorganic-organic perovskites (CH<sub>3</sub>NH<sub>3</sub>) PbX<sub>3</sub> and CsPbX<sub>3</sub> (X = Cl, Br, I). *J. Korean Phys. Soc.* **2004**, *44*, 889–893.
35. Frost, J.M.; Butler, K.T.; Brivio, F.; Hendon, C.H.; van Schilfegaarde, M.; Walsh, A. Atomistic origins of high-performance in hybrid halide perovskite solar cells. *Nano Lett.* **2014**, *14*, 2584–2590. [[CrossRef](#)]
36. Brivio, F.; Walker, A.B.; Walsh, A. Structural and electronic properties of hybrid perovskites for high-efficiency thin-film photovoltaics from first-principles. *Apl Mater.* **2013**, *1*, 042111. [[CrossRef](#)]
37. Umari, P.; Mosconi, E.; De Angelis, F. Relativistic GW calculations on CH<sub>3</sub>NH<sub>3</sub>PbI<sub>3</sub> and CH<sub>3</sub>NH<sub>3</sub>SnI<sub>3</sub> perovskites for solar cell applications. *Sci. Rep.* **2014**, *4*, 4467. [[CrossRef](#)]
38. Jeon, N.-J.; Noh, J.-H.; Kim, Y.-C.; Yang, W.-S.; Ryu, S.-C.; Seok, S.-I. Solvent engineering for high-performance inorganic–organic hybrid perovskite solar cells. *Nat. Mater.* **2014**, *13*, 897–903. [[CrossRef](#)]
39. Zhou, H.; Chen, Q.; Li, G.; Luo, S.; Song, T.-B.; Duan, H.-S.; Hong, Z.; Jingbi You, J.; Liu, Y.; Yang, Y. Interface engineering of highly efficient perovskite solar cells. *Science* **2014**, *345*, 542–546. [[CrossRef](#)]
40. Shin, S.-S.; Yeom, E.-J.; Yang, W.-S.; Hur, S.; Kim, M.-G.; Im, J.; Seo, J.-W.; Noh, J.-H.; Seok, S.-I. Colloidally prepared La-doped BaSnO<sub>3</sub> electrodes for efficient, photostable perovskite solar cells. *Science* **2017**, *356*, 167–171. [[CrossRef](#)] [[PubMed](#)]
41. Yin, W.-J.; Yang, J.-H.; Kang, J.-G.; Yan, Y.; Wei, S.-H. Halide perovskite materials for solar cells: A theoretical review. *J. Mater. Chem. A* **2015**, *3*, 8926–8942. [[CrossRef](#)]
42. Wang, Y.; Duan, C.; Lv, P.; Ku, Z.; Lu, J.; Huang, F.; Cheng, Y.-B. Printing strategies for scaling-up perovskite solar cells. *Natl. Sci. Rev.* **2021**, *8*, nwab075. [[CrossRef](#)]
43. Saki, Z.; Byranvand, M.M.; Taghavinia, N.; Kedia, M.; Saliba, M. Solution-processed perovskite thin-films: The journey from lab-to large-scale solar cells. *Energy Environ. Sci.* **2021**, *14*, 5690. [[CrossRef](#)]
44. Chen, C.-S.; Ran, C.; Yao, Q.; Wang, J.; Guo, C.; Gu, L.; Han, H.; Wang, X.; Chao, L.; Xia, Y.; et al. Screen-Printing Technology for Scale Manufacturing of Perovskite Solar Cells. *Adv. Sci.* **2023**, 2303992. [[CrossRef](#)] [[PubMed](#)]
45. Swarnkar, A.; Marshall, A.R.; Sanehira, E.M.; Chernomordik, B.D.; Moore, D.T.; Christians, J.A.; Chakrabarti, T.; Luther, J.M. Quantum dot–induced phase stabilization of  $\alpha$ -CsPbI<sub>3</sub> perovskite for high-efficiency photovoltaics. *Science* **2016**, *354*, 92–95. [[CrossRef](#)]
46. Wang, P.; Zhang, X.; Zhou, Y.; Jiang, Q.; Ye, Q.; Chu, Z.; Li, X.; Yang, X.; Yin, Z.; You, J. Solvent-controlled growth of inorganic perovskite films in dry environment for efficient and stable solar cells. *Nat. Commun.* **2018**, *9*, 2225. [[CrossRef](#)]
47. Wang, Y.; Zhang, T.; Kan, M.; Zhao, Y. Bifunctional stabilization of all-inorganic  $\alpha$ -CsPbI<sub>3</sub> perovskite for 17% efficiency photovoltaics. *J. Am. Chem. Soc.* **2018**, *140*, 12345–12348. [[CrossRef](#)]
48. Liu, C.; Li, W.; Zhang, C.; Ma, Y.; Fan, J.; Mai, Y. All-inorganic CsPbI<sub>2</sub>Br perovskite solar cells with high efficiency exceeding 13%. *J. Am. Chem. Soc.* **2018**, *140*, 3825–3828. [[CrossRef](#)]
49. Liu, C.; Li, W.; Li, H.; Wang, H.; Zhang, C.; Yang, Y.; Gao, X.; Xue, Q.; Yip, H.-L.; Fan, J.; et al. Structurally Reconstructed CsPbI<sub>2</sub>Br Perovskite for Highly Stable and Square-Centimeter All-Inorganic Perovskite Solar Cells. *Adv. Energy Mater.* **2019**, *9*, 1803572. [[CrossRef](#)]
50. Wang, J.; Zhang, J.; Zhou, Y.; Liu, H.; Xue, Q.; Li, X.; Chueh, C.-C.; Yip, H.-L.; Zhu, Z.; Jen, A.K.Y. Highly efficient all-inorganic perovskite solar cells with suppressed non-radiative recombination by a Lewis base. *Nat. Commun.* **2020**, *11*, 177.
51. Luévano-Hipólito, E.; Quintero-Lizárraga, O.L.; Torres-Martínez, L.M. A Critical Review of the Use of Bismuth Halide Perovskites for CO<sub>2</sub> Photoreduction: Stability Challenges and Strategies Implemented. *Catalysts* **2022**, *12*, 1410. [[CrossRef](#)]
52. Chen, X.; Jia, M.; Xu, W.; Pan, G.; Zhu, J.; Tian, Y.; Wu, D.; Li, X.; Shi, Z. Recent Progress and Challenges of Bismuth-Based Halide Perovskites for Emerging Optoelectronic Applications. *Adv. Opt. Mater.* **2022**, *11*, 2202153.
53. Stoumpos, C.C.; Malliakas, C.D.; Kanatzidis, M.G. Semiconducting tin and lead iodide perovskites with organic cations: Phase transitions, high mobilities, and near-infrared photoluminescent properties. *Inorg. Chem.* **2013**, *52*, 9019–9038. [[PubMed](#)]
54. Xing, G.; Mathews, N.; Lim, S.S.; Yantara, N.; Liu, X.; Sabba, D.; Grätzel, M.; Mhaisalkar, S.; Sum, T.C. Low-temperature solution-processed wavelength-tunable perovskites for lasing. *Nat. Mater.* **2014**, *13*, 476–480. [[CrossRef](#)]
55. Miyata, A.; Mitioglu, A.; Plochocka, P.; Portugall, O.; Wang, J.T.-W.; Stranks, S.D.; Snaith, H.J.; Nicholas, R.J. Direct measurement of the exciton binding energy and effective masses for charge carriers in organic–inorganic tri-halide perovskites. *Nat. Phys.* **2015**, *11*, 582–587.
56. Noda-Yamamuro, N.; Matsuo, T.; Suga, H. Dielectric study of CH<sub>3</sub>NH<sub>3</sub>PbX<sub>3</sub> (X = Cl, Br, I). *J. Phys. Chem. Solids* **1992**, *53*, 935–939. [[CrossRef](#)]
57. Sanehira, E.M.; Marshall, A.R.; Christians, J.A.; Harvey, S.P.; Ciesielski, P.N.; Wheeler, L.M.; Schulz, P.; Lin, L.Y.; Beard, M.C.; Luther, J.M. Enhanced mobility CsPbI<sub>3</sub> quantum dot arrays for record-efficiency, high-voltage photovoltaic cells. *Sci. Adv.* **2017**, *3*, eaao4204.
58. Christians, J.A.; Fung, R.C.M.; Kamat, P.V. An inorganic hole conductor for organo-lead halide perovskite solar cells. Improved hole conductivity with copper iodide. *J. Am. Chem. Soc.* **2014**, *136*, 758–764.
59. Subbiah, A.S.; Halder, A.; Ghosh, S.; Mahuli, N.; Hodes, G.; Sarkar, S.K. Inorganic hole conducting layers for perovskite-based solar cells. *J. Phys. Chem. Lett.* **2014**, *5*, 1748–1753. [[PubMed](#)]

60. Qin, P.; Tanaka, S.; Ito, S.; Tetreault, N.; Manabe, K.; Nishino, H.; Nazeeruddin, M.K.; Grätzel, M. Inorganic hole conductor-based lead halide perovskite solar cells with 12.4% conversion efficiency. *Nat. Commun.* **2014**, *5*, 3834. [[PubMed](#)]
61. Yin, X.; Chen, P.; Que, M.; Xing, Y.; Que, W.; Niu, C.; Shao, J. Highly efficient flexible perovskite solar cells using solution-derived NiOx hole contacts. *ACS Nano* **2016**, *10*, 3630–3636.
62. Ruhle, S. Tabulated values of the Shockley–Queisser limit for single junction solar cell. *Sol. Energy* **2016**, *130*, 139–147. [[CrossRef](#)]
63. Nazeeruddin, M.K.; Snaith, H. Methylammonium lead triiodide perovskite solar cells: A new paradigm in photovoltaics. *Mrs Bull.* **2015**, *40*, 641–645. [[CrossRef](#)]
64. Yuan, H.; Debroye, E.; Janssen, K.; Naiki, H.; Steuwe, C.; Lu, G.; Moris, M.; Orgiu, E.; Uji-i, H.; De Schryver, F.; et al. Degradation of Methylammonium Lead Iodide Perovskite Structures through Light and Electron Beam Driven Ion Migration. *J. Phys. Chem. Lett.* **2016**, *7*, 561–566. [[CrossRef](#)]
65. Juarez-Perez, E.J.; Ono, L.K.; Qi, Y. Thermal degradation of formamidinium based lead halide perovskites into *sym*-triazine and hydrogen cyanide observed by coupled thermogravimetry-mass spectrometry analysis. *J. Mater. Chem. A* **2019**, *7*, 16912–16919. [[CrossRef](#)]
66. Yadegarifard, A.; Lee, H.; Seok, H.-J.; Kim, I.; Ju, B.-K.; Kim, H.-K.; Lee, D.-K. FA/Cs-based mixed Pb–Sn perovskite solar cells: A review of recent advances in stability and efficiency. *Nano Energy* **2023**, *112*, 108481. [[CrossRef](#)]
67. Li, M.; Sun, R.; Chang, J.; Dong, J.; Tian, Q.; Wang, H.; Li, Z.; Yang, P.; Shi, H.; Yang, C.; et al. Orientated crystallization of FA-based perovskite via hydrogen-bonded polymer network for efficient and stable solar cells. *Nat. Commun.* **2023**, *14*, 573. [[CrossRef](#)]
68. Zhao, Y.; Tan, H.; Yuan, H.; Yang, Z.; Fan, J.Z.; Kim, J.-H.; Voznyy, O.; Gong, X.; Quan, L.N.; Tan, C.S.; et al. Perovskite seeding growth of formamidinium-lead-iodide-based perovskites for efficient and stable solar cells. *Nat. Commun.* **2018**, *9*, 1607. [[CrossRef](#)]
69. Pellet, N.; Gao, P.; Gregori, G.; Yang, T.Y.; Nazeeruddin, M.K.; Maier, J.; Grätzel, M. Mixed-Organic-Cation Perovskite Photovoltaics for Enhanced Solar-Light Harvesting. *Angew. Chem. Int. Ed.* **2014**, *53*, 3151–3157. [[CrossRef](#)]
70. Lee, J.W.; Seol, D.J.; Cho, A.N.; Park, N.G. High-Efficiency Perovskite Solar Cells Based on the Black Polymorph of  $\text{HC}(\text{NH}_2)_2\text{PbI}_3$ . *Adv. Mater.* **2014**, *26*, 4991–4998. [[CrossRef](#)] [[PubMed](#)]
71. Lee, J.W.; Kim, D.H.; Kim, H.S.; Seo, S.W.; Cho, S.M.; Park, N.G. Formamidinium and Cesium Hybridization for Photo- and Moisture-Stable Perovskite Solar Cell. *Adv. Energy Mater.* **2015**, *5*, 1501310. [[CrossRef](#)]
72. Kim, M.; Kim, G.-H.; Lee, T.K.; Choi, I.W.; Choi, H.W.; Jo, Y.; Yoon, Y.J.; Kim, J.W.; Lee, J.; Huh, D.; et al. Methylammonium Chloride Induces Intermediate Phase Stabilization for Efficient Perovskite Solar Cells. *Joule* **2019**, *3*, 2179–2192. [[CrossRef](#)]
73. Yao, Q.; Xue, Q.; Li, Z.; Zhang, K.; Zhang, T.; Li, N.; Yang, S.; Brabec, C.J.; Yip, H.-L.; Cao, Y. Graded 2D/3D Perovskite Heterostructure for Efficient and Operationally Stable MA-Free Perovskite Solar Cells. *Adv. Mater.* **2020**, *32*, 2000571. [[CrossRef](#)]
74. Wang, Y.; Mahmoudi, T.; Hahn, Y.-B. Highly stable and Efficient Perovskite Solar Cells Based on FAMA-Perovskite-Cu:NiO Composites with 20.7% Efficiency and 80.5% Fill Factor. *Adv. Energy Mater.* **2020**, *10*, 2000967. [[CrossRef](#)]
75. Wang, Q.; Tang, W.; Chen, Y.; Qiu, W.; Wu, Y.; Peng, Q. Over 25% efficiency and stable bromine-free RbCsFAMA-based quadruple cation perovskite solar cells enabled by an aromatic zwitterion. *J. Mater. Chem. A* **2023**, *11*, 1170. [[CrossRef](#)]
76. Wang, Y.; Li, W.; Zhang, T.Y.; Li, D.H.; Kan, M.; Wang, X.T.; Liu, X.M.; Wang, T.; Zhao, Y.X. Highly efficient (110) orientated FA-MA mixed cation perovskite solar cells via functionalized carbon nanotube and methylammonium chloride additive. *Small Methods* **2019**, *4*, 1900511. [[CrossRef](#)]
77. Jeon, N.J.; Noh, J.H.; Yang, W.S.; Kim, Y.C.; Ryu, S.; Seo, S.; Seok, S.I. Compositional engineering of perovskite materials for high-performance solar cells. *Nature* **2015**, *517*, 476–480. [[CrossRef](#)]
78. Wu, Y.; Yang, X.; Chen, W.; Yue, Y.; Cai, M.; Xie, F.; Bi, E.; Islam, A.; Han, L. Perovskite solar cells with 18.21% efficiency and area over  $1\text{cm}^2$  fabricated by heterojunction engineering. *Nat. Energy* **2016**, *1*, 16148. [[CrossRef](#)]
79. Li, F.; Hou, X.; Wang, Z.; Cui, X.; Xie, G.; Yan, F.; Zhao, X.-Z.; Tai, Q. FA/MA Cation Exchange for Efficient and Reproducible Tin-Based Perovskite Solar Cells. *ACS Appl. Mater. Interfaces* **2021**, *13*, 40656–40663. [[CrossRef](#)] [[PubMed](#)]
80. Wang, M.; Wang, W. High-efficiency and stable  $\text{FA}_{0.75}\text{MA}_{0.25}\text{SnI}_3$  perovskite solar cells with large-size crystal grains prepared by doping with multifunctional chloride salt. *New J. Chem.* **2023**, *47*, 15666–15676. [[CrossRef](#)]
81. Zhao, Z.; Gu, F.; Li, Y.; Sun, W.; Ye, S.; Rao, H.; Liu, Z.; Bian, Z.; Huang, C. Mixed-organic-cation tin iodide for lead-free perovskite solar cells with an efficiency of 8.12%. *Adv. Sci.* **2017**, *4*, 1700204. [[CrossRef](#)] [[PubMed](#)]
82. Jin, Z.; Yu, B.B.; Liao, M.; Liu, D.; Xiu, J.; Zhang, Z.; Lifshitz, E.; Tang, J.; Song, H.; He, Z. Enhanced efficiency and stability in Sn-based perovskite solar cells with secondary crystallization growth. *J. Energy Chem.* **2021**, *54*, 414–421. [[CrossRef](#)]
83. Kim, M.; Kim, G.H.; Oh, K.S.; Jo, Y.; Yoon, H.; Kim, K.H.; Lee, H.; Kim, J.Y.; Kim, D.S. High-Temperature–Short-Time Annealing Process for High-Performance Large-Area Perovskite Solar Cells. *ACS Nano* **2017**, *11*, 6057–6064. [[CrossRef](#)] [[PubMed](#)]
84. Jiang, Q.; Chu, Z.; Wang, P.; Yang, X.; Liu, H.; Wang, Y.; Yin, Z.; Wu, J.; Zhang, X.; You, J. Planar-Structure Perovskite Solar Cells with Efficiency beyond 21%. *Adv. Mater.* **2017**, *29*, 1703852. [[CrossRef](#)]
85. Tan, H.; Jain, A.; Voznyy, O.; Lan, X.; Garcia de Arquer, F.P.; Fan, J.Z.; Quintero-Bermudez, R.; Yuan, M.; Zhang, B.; Zhao, Y.; et al. Efficient and stable solution-processed planar perovskite solar cells via contact passivation. *Science* **2017**, *355*, 722–726. [[CrossRef](#)]
86. Du, J.; Feng, L.; Guo, X.; Huang, X.; Lin, Z.; Su, J.; Hao, Y. Enhanced efficiency and stability of planar perovskite solar cells by introducing amino acid to  $\text{SnO}_2$ /perovskite interface. *J. Power Sources* **2020**, *455*, 227974. [[CrossRef](#)]
87. Bu, T.; Wu, L.; Liu, X.; Yang, X.; Zhou, P.; Yu, X.; Qin, T.; Shi, J.; Wang, S.; Li, S.; et al. Synergic interface optimization with green solvent engineering in mixed perovskite solar cells. *Adv. Energy Mater.* **2017**, *7*, 1700576. [[CrossRef](#)]

88. Jeon, N.J.; Na, H.; Jung, E.H.; Yang, T.; Lee, Y.G.; Kim, G.; Shin, H.; Seok, S.I.; Lee, J.; Seo, J. A fluorene-terminated hole-transporting material for highly efficient and stable perovskite solar cells. *Nat. Energy* **2018**, *3*, 682–689. [CrossRef]
89. Yoo, J.J.; Wieghold, S.; Sponseller, M.C.; Chua, M.R.; Bertram, S.N.; Hartono, N.T.P.; Tresback, J.S.; Hansen, E.C.; Correa-Baena, J.-P.; Bulović, V.; et al. An interface stabilized perovskite solar cell with high stabilized efficiency and low voltage loss. *Energy Environ. Sci.* **2019**, *12*, 2192–2199. [CrossRef]
90. Al-Ashouri, A.; Magomedov, A.; Roß, M.; Jošt, M.; Talaikis, M.; Chistiakova, G.; Bertram, T.; Márquez, J.A.; Köhnen, E.; Kasparavičius, E.; et al. Conformal monolayer contacts with lossless interfaces for perovskite single junction and monolithic tandem solar cells. *Energy Environ. Sci.* **2019**, *12*, 3356–3369. [CrossRef]
91. Kim, D.-H.; Muzzillo, C.P.; Tong, J.; Palmstrom, A.F.; Larson, B.W.; Choi, C.-S.; Harvey, S.P.; Glynn, S.; Whitaker, J.B.; Zhang, F.; et al. Bimolecular Additives Improve Wide-Band-Gap Perovskites for Efficient Tandem Solar Cells with CIGS. *Joule* **2019**, *3*, 1734–1745. [CrossRef]
92. Tong, J.; Song, Z.; Kim, D.H.; Chen, X.; Chen, C.; Palmstrom, A.F.; Ndione, P.F.; Reese, M.O.; Dunfield, S.P.; Reid, O.G.; et al. Carrier lifetimes of >1  $\mu$ s in Sn-Pb perovskites enable efficient all-perovskite tandem solar cells. *Science* **2019**, *364*, 475–479. [CrossRef]
93. Xiao, K.; Lin, Y.-H.; Zhang, M.; Oliver, R.D.J.; Wang, X.; Liu, Z.; Luo, X.; Li, J.; Lai, D.; Luo, H.; et al. Scalable processing for realizing 21.7%-efficient all-perovskite tandem solar modules. *Science* **2022**, *376*, 762–767. [CrossRef]
94. Kim, H.-S.; Lee, J.-W.; Yantara, N.; Boix, P.P.; Kulkarni, S.A.; Mhaisalkar, S.; Grätzel, M.; Park, N.G. High efficiency solid-state sensitized solar cell-based on submicrometer rutile TiO<sub>2</sub> nanorod and CH<sub>3</sub>NH<sub>3</sub>PbI<sub>3</sub> perovskite sensitizer. *Nano Lett.* **2013**, *13*, 2412–2417. [CrossRef]
95. Etgar, L.; Gao, P.; Xue, Z.; Peng, Q.; Chandiran, A.K.; Liu, B.; Nazeeruddin, M.K.; Grätzel, M. Mesoscopic CH<sub>3</sub>NH<sub>3</sub>PbI<sub>3</sub>/TiO<sub>2</sub> heterojunction solar cells. *J. Am. Chem. Soc.* **2012**, *134*, 17396–17399. [CrossRef]
96. Cho, H.; Jeong, S.-H.; Park, M.-H.; Kim, Y.-H.; Wolf, C.; Lee, C.-L.; Heo, J.-H.; Sadhanala, A.; Myoung, N.; Yoo, S.-H.; et al. Overcoming the electroluminescence efficiency limitations of perovskite light-emitting diodes. *Science* **2015**, *350*, 1222–1225. [CrossRef]
97. Gauthron, K.; Lauret, J.S.; Doyennette, L.; Lanty, G.; Al Choueiry, A.; Zhang, S.J.; Brehier, A.; Largeau, L.; Mauguin, O.; Bloch, J.; et al. Optical spectroscopy of two-dimensional layered (C<sub>6</sub>H<sub>5</sub>C<sub>2</sub>H<sub>4</sub>-NH<sub>3</sub>)<sub>2</sub>-PbI<sub>4</sub> perovskite. *Opt. Express* **2010**, *18*, 5912–5919. [CrossRef]
98. Chen, Q.; Zhou, H.; Hong, Z.; Luo, S.; Duan, H.-S.; Wang, H.-H.; Liu, Y.; Li, G.; Yang, Y. Planar heterojunction perovskite solar cells via vapor-assisted solution process. *J. Am. Chem. Soc.* **2014**, *136*, 622–625. [CrossRef] [PubMed]
99. Baikie, T.; Fang, Y.; Kadro, J.M.; Schreyer, M.; Wei, F.; Mhaisalkar, S.G.; Graetzel, M.; White, T.J. Synthesis and crystal chemistry of the hybrid perovskite (CH<sub>3</sub>NH<sub>3</sub>) PbI<sub>3</sub> for solid-state sensitised solar cell applications. *J. Mater. Chem. A* **2013**, *1*, 5628–5641. [CrossRef]
100. Sum, T.C.; Mathews, N. Advancements in perovskite solar cells: Photophysics behind the photovoltaics. *Energy Environ. Sci.* **2014**, *7*, 2518–2534. [CrossRef]
101. Ponseca, C.S., Jr.; Savenije, T.J.; Abdellah, M.; Zheng, K.; Yartsev, A.; Pascher, T.; Harlang, T.; Chabera, P.; Pullerits, T.; Stepanov, A.; et al. Organometal halide perovskite solar cell materials rationalized: Ultrafast charge generation, high and microsecond-long balanced mobilities, and slow recombination. *J. Am. Chem. Soc.* **2014**, *136*, 5189–5192. [CrossRef]
102. Mosconi, E.; Amat, A.; Nazeeruddin, M.K.; Grätzel, M.; De Angelis, F. First-principles modeling of mixed halide organometal perovskites for photovoltaic applications. *J. Phys. Chem. C* **2013**, *117*, 13902–13913. [CrossRef]
103. Koutselas, I.B.; Ducasse, L.; Papavassiliou, G.C. Electronic properties of three- and low-dimensional semiconducting materials with Pb halide and Sn halide units. *J. Phys. Condens. Matter* **1996**, *8*, 1217–1227. [CrossRef]
104. Zhang, M.; Yu, H.; Lyu, M.; Wang, Q.; Yun, J.-H.; Wang, L. Composition-dependent photoluminescence intensity and prolonged recombination lifetime of perovskite CH<sub>3</sub>NH<sub>3</sub>PbBr<sub>(3-x)</sub>Cl<sub>x</sub> films. *Chem. Commun.* **2014**, *50*, 11727–11730. [CrossRef]
105. Cai, B.; Xing, Y.; Yang, Z.; Zhang, W.-H.; Qiu, J. High performance hybrid solar cells sensitized by organolead halide perovskites. *Energy Environ. Sci.* **2013**, *6*, 1480–1485. [CrossRef]
106. Zhang, J.; Yin, C.; Yang, F.; Yao, Y.; Yuan, F.; Chen, H.; Wang, R.; Bai, S.; Tu, G.; Hou, L. Highly Luminescent and Stable CsPbI<sub>3</sub> Perovskite Nanocrystals with Sodium Dodecyl Sulfate Ligand Passivation for Red-Light-Emitting Diodes. *J. Phys. Chem. Lett.* **2021**, *12*, 2437–2443. [CrossRef]
107. Cheng, Y.; Ding, L. Perovskite/Si Tandem Solar Cells: Fundamentals, Advances, Challenges, and Novel Applications. *Sus. Mat.* **2021**, *1*, 324–344. [CrossRef]
108. Mailoa, J.P.; Bailie, C.D.; Johlin, E.C.; Hoke, E.T.; Akey, A.J.; Nguyen, W.H.; McGehee, M.D.; Buonassisi, T. A 2-terminal perovskite/silicon multijunction solar cell enabled by a silicon tunnel junction. *Appl. Phys. Lett.* **2015**, *106*, 121105. [CrossRef]
109. Tandem Solar Cell Achieves 32.5 Percent Efficiency. *Science Daily*. 19 December 2022. Available online: <https://www.sciencedaily.com/releases/2022/12/221219164845.htm> (accessed on 12 July 2023).
110. Oxford PV Sets New Solar Cell World Record. *Oxford PV*. 24 May 2023. Available online: <https://www.oxfordpv.com/news/oxford-pv-sets-new-solar-cell-world-record> (accessed on 12 July 2023).
111. KAUST Claims 33.7% Efficiency for Perovskite/Silicon Tandem Solar Cell. *PV Magazine*. 30 May 2023. Available online: <https://www.pv-magazine.com/2023/05/30/kaust-claims-33-7-efficiency-for-perovskite-silicon-tandem-solar-cell/> (accessed on 12 July 2023).

112. LONGI. 2023. Available online: <https://www.longi.com/en/news/new-conversion-efficiency/> (accessed on 12 July 2023).
113. Chin, X.Y.; Turkyay, D.; Steele, J.A.; Tabean, S.; Eswara, S.; Mensi, M.; Fiala, P.; Wolff, C.M.; Paracchino, A.; Artuk, K.; et al. Interface passivation for 31.25%-efficient perovskite/silicon tandem solar cells. *Science* **2023**, *381*, 59–63. [[CrossRef](#)] [[PubMed](#)]
114. Lee, B.-H.; Stoumpos, C.C.; Zhou, N.; Hao, F.; Malliakas, C.; Yeh, C.Y.; Marks, T.J.; Kanatzidis, M.G.; Chang, R.P.H. Air-stable molecular semiconducting iodosalts for solar cell applications: Cs<sub>2</sub>SnI<sub>6</sub> as a hole conductor. *J. Am. Chem. Soc.* **2014**, *136*, 15379–15385. [[CrossRef](#)]
115. Maughan, A.E.; Ganose, A.M.; Bordelon, M.M.; Miller, E.M.; Scanlon, D.O.; Neilson, J.R. Defect tolerance to intolerance in the vacancy-ordered double perovskite semiconductors Cs<sub>2</sub>SnI<sub>6</sub> and Cs<sub>2</sub>TeI<sub>6</sub>. *J. Am. Chem. Soc.* **2016**, *138*, 8453–8464. [[CrossRef](#)] [[PubMed](#)]
116. Kaltzoglou, A.; Antoniadou, M.; Kontos, A.G.; Stoumpos, C.C.; Perganti, D.; Siranidi, E.; Raptis, V.; Trohidou, K.; Psycharis, V.; Kanatzidis, M.G.; et al. Optical-vibrational properties of the Cs<sub>2</sub>SnX<sub>6</sub> (X = Cl, Br, I) defect perovskites and hole-transport efficiency in dye-sensitized solar cells. *J. Phys. Chem. C* **2016**, *120*, 11777–11785. [[CrossRef](#)]
117. Kadro, J.M.; Pellet, N.; Giordano, F.; Ulianov, A.; Müntener, O.; Maier, J.; Grätzel, M.; Hagfeldt, A. Proof-of-concept for facile perovskite solar cell recycling. *Energy Environ. Sci.* **2016**, *9*, 3172–3179. [[CrossRef](#)]
118. Tsai, C.-M.; Mohanta, N.; Wang, C.-Y.; Lin, Y.-P.; Yang, Y.-W.; Wang, C.-L.; Hung, C.-H.; Diao, E.W.-G. Formation of Stable Tin Perovskites Co-crystallized with Three Halides for Carbon-Based Mesoscopic Lead-Free Perovskite Solar Cells. *Angew. Chem. Int. Ed.* **2017**, *56*, 13819–13823. [[CrossRef](#)] [[PubMed](#)]
119. Sabba, D.; Mulmudi, H.K.; Prabhakar, R.R.; Krishnamoorthy, T.; Baikie, T.; Boix, P.P.; Mhaisalkar, S.; Mathews, N. Impact of anionic Br-substitution on open circuit voltage in lead free perovskite (CsSnI<sub>3-x</sub>Br<sub>x</sub>) solar cells. *J. Phys. Chem. C* **2015**, *119*, 1763–1767. [[CrossRef](#)]
120. Dong, H.; Ran, C.; Gao, W.; Sun, N.; Liu, X.; Xia, Y.; Chen, Y.; Huang, W. Crystallization Dynamics of Sn-Based Perovskite Thin Films: Toward Efficient and Stable Photovoltaic Devices. *Adv. Energy Mater.* **2022**, *12*, 2102213. [[CrossRef](#)]
121. Mohammadian-Sarcheshmeh, H.; Mazloun-Ardakani, M.; Rameez, M.; Shahbazi, S.; Diao, E.W.-G. Application of a natural antioxidant as an efficient strategy to decrease the oxidation in Sn-based perovskites. *J. Alloys Compd.* **2020**, *846*, 156351. [[CrossRef](#)]
122. Wang, M.; Wang, W.; Shen, Y.; Cao, K.; Chen, J.; Zhao, X.; Xie, M.; Chen, S. Suppression of Sn<sup>2+</sup> oxidation and formation of large-size crystal grains with multifunctional chloride salt for perovskite solar cell applications. *J. Mater. Chem. C* **2022**, *10*, 10669–10678. [[CrossRef](#)]
123. Mahmoudi, T.; Rho, W.-Y.; Kohan, M.; Im, Y.H.; Mathur, S.; Hahn, Y.-B. Suppression of Sn<sup>2+</sup>/Sn<sup>4+</sup> oxidation in tin-based perovskite solar cells with graphene-tin quantum dots composites in active layer. *Nano Energy* **2021**, *90 Pt A*, 106495. [[CrossRef](#)]
124. Ma, Z.; Peng, S.; Wu, Y.; Fang, X.; Chen, X.; Jia, X.; Zhang, K.; Yuan, N.; Ding, J.; Dai, N. Air-stable layered bismuth-based perovskite-like materials: Structures and semiconductor properties. *Phys. B Condens. Matter* **2017**, *526*, 136–142. [[CrossRef](#)]
125. Jain, S.M.; Phuyal, D.; Davies, M.L.; Li, M.; Philippe, B.; De Castro, C.; Qiu, Z.; Kim, J.-H.; Watson, T.; Tsoi, W.C.; et al. An effective approach of vapour assisted morphological tailoring for reducing metal defect sites in lead-free, (CH<sub>3</sub>NH<sub>3</sub>)<sub>3</sub>Bi<sub>2</sub>I<sub>9</sub> bismuth-based perovskite solar cells for improved performance and long-term stability. *Nano Energy* **2018**, *49*, 614–624. [[CrossRef](#)]
126. Zhang, Z.; Li, X.; Xia, X.; Wang, Z.; Huang, Z.; Lei, B.; Gao, Y. High-quality (CH<sub>3</sub>NH<sub>3</sub>)<sub>3</sub>Bi<sub>2</sub>I<sub>9</sub> film-based solar cells: Pushing efficiency up to 1.64%. *J. Phys. Chem. Lett.* **2017**, *8*, 4300–4307. [[CrossRef](#)] [[PubMed](#)]
127. Lan, C.; Liang, G.; Zhao, S.; Lan, H.; Peng, H.; Zhang, D.; Sun, H.; Luo, J.; Fan, P. Lead-free formamidinium bismuth perovskites (FA)<sub>3</sub>Bi<sub>2</sub>I<sub>9</sub> with low bandgap for potential photovoltaic application. *Sol. Energy* **2019**, *177*, 501–507. [[CrossRef](#)]
128. Ahmad, K.; Mobin, S.M. Recent Progress and Challenges in A<sub>3</sub>Sb<sub>2</sub>X<sub>9</sub>-Based Perovskite Solar Cells. *ACS Omega* **2020**, *5*, 28404–28412. [[CrossRef](#)]
129. Guo, Y.; Zhao, F.; Yang, P.; Gao, M.; Shen, J.; Tao, J.; Jiang, J.; Chu, J. DMAI-driven all-inorganic antimony-based perovskite-inspired solar cells with record open-circuit voltage. *J. Mater. Chem. A* **2023**, *11*, 6474. [[CrossRef](#)]
130. Xiang, S.; Li, W.; Wei, Y.; Liu, J.; Liu, H.; Zhu, L.; Chen, H. The synergistic effect of non-stoichiometry and Sb-doping on air-stable α-CsPbI<sub>3</sub> for efficient carbon-based perovskite solar cells. *Nanoscale* **2018**, *10*, 9996. [[CrossRef](#)]
131. Al-Anesi, B.; Grandhi, G.K.; Pecoraro, A.; Sugathan, V.; Viswanath, N.S.M.; Ali-Löytty, H.; Liu, M.; Ruoko, T.-P.; Lahtonen, K.; Manna, D.; et al. Antimony-bismuth alloying: The key to a major boost in the efficiency of lead-free perovskite-inspired indoor photovoltaics. *ChemRxiv* **2023**, 2303575. [[CrossRef](#)]
132. Nie, R.; Mehta, A.; Park, B.-W.; Kwon, H.-W.; Im, J.; Seok, S.-I. Mixed sulfur and iodide-based lead-free perovskite solar cells. *J. Am. Chem. Soc.* **2018**, *140*, 872–875. [[CrossRef](#)] [[PubMed](#)]
133. Grandhi, G.K.; Jagadamma, L.K.; Sugathan, V.; Al-Anesi, B.; Manna, D.; Vivo, P. Lead-free perovskite-inspired semiconductors for indoor light-harvesting—The present and the future. *Chem. Commun.* **2023**, *59*, 8616–8625. [[CrossRef](#)] [[PubMed](#)]
134. Stoumpos, C.C.; Frazer, L. Hybrid germanium iodide perovskite semiconductors: Active lone pairs, structural distortion, Direct and Indirect energy gaps, and strong nonlinear optical properties. *J. Am. Chem. Soc.* **2015**, *137*, 6804–6819. [[CrossRef](#)] [[PubMed](#)]
135. Krishnamoorthy, T.; Ding, H.; Yan, C.; Leong, W.L.; Baikie, T.; Zhang, Z.; Sherburne, M.; Li, S.; Asta, M.; Mathews, N.; et al. Lead-free germanium iodide perovskite materials for photovoltaic applications. *J. Mater. Chem. A* **2015**, *3*, 23829–23832. [[CrossRef](#)]
136. Chatterjee, S.; Pal, A.J. Tin (IV) substitution in (CH<sub>3</sub>NH<sub>3</sub>)<sub>3</sub>Sb<sub>2</sub>I<sub>9</sub>: Toward low-band-gap defect-ordered hybrid perovskite solar cells. *ACS Appl. Mater. Interfaces* **2018**, *10*, 35194–35205. [[CrossRef](#)]
137. Kopacic, I.; Friesenbichler, B.; Hoefler, S.F.; Kunert, B.; Plank, H.; Rath, T.; Trimmel, G. Enhanced performance of germanium halide perovskite solar cells through compositional engineering. *ACS Appl. Energy Mater.* **2018**, *1*, 343–347. [[CrossRef](#)]

138. Slavney, A.H.; Leppert, L.; Bartesaghi, D.; Gold-Parker, A.; Toney, M.F.; Savenije, T.J.; Neaton, J.B.; Karunadasa, H.I. Defect-induced band-edge reconstruction of a bismuth-halide double perovskite for visible-light absorption. *J. Am. Chem. Soc.* **2017**, *139*, 5015–5018. [[CrossRef](#)]
139. McClure, E.T.; Ball, M.R.; Windl, W.; Woodward, P.M. Cs<sub>2</sub>AgBiX<sub>6</sub> (X = Br, Cl): New visible light absorbing, lead-free halide perovskite semiconductors. *Chem. Mater.* **2016**, *28*, 1348–1354. [[CrossRef](#)]
140. Wei, F.; Deng, Z.; Sun, S.; Xie, F.; Kieslich, G.; Evans, D.M.; Carpenter, M.A.; Bristowe, P.W.; Cheetham, A.K. The synthesis, structure and electronic properties of a lead-free hybrid inorganic–organic double perovskite (MA)<sub>2</sub>KBiCl<sub>6</sub> (MA = methylammonium). *Mater. Horiz.* **2016**, *3*, 328–332. [[CrossRef](#)]
141. Zhao, X.-G.; Yang, J.-H.; Fu, Y.; Yang, D.; Xu, Q.; Yu, L.; Wei, S.-H.; Zhang, L. Design of lead-free inorganic halide perovskites for solar cells via cation-transmutation. *J. Am. Chem. Soc.* **2017**, *139*, 2630–2638. [[CrossRef](#)] [[PubMed](#)]
142. Tiwari, D.; Hutter, O.S.; Longo, G. Chalcogenide perovskites for photovoltaics: Current status and prospects. *J. Phys. Energy* **2021**, *3*, 034010. [[CrossRef](#)]
143. Nishigaki, Y.; Nagai, T.; Nishiwaki, M.; Aizawa, T.; Kozawa, M.; Hanzawa, K.; Kato, Y.; Sai, H.; Hiramatsu, H.; Hosono, H.; et al. Extraordinary strong band-edge absorption in distorted chalcogenide perovskites. *Sol. RRL* **2020**, *4*, 1900555. [[CrossRef](#)]
144. Ayaydah, W.; Raddad, E.; Hawash, Z. Sn-Based Perovskite Solar Cells towards High Stability and Performance. *Micromachines* **2023**, *14*, 806. [[CrossRef](#)] [[PubMed](#)]
145. Xiao, K.; Lin, R.; Han, Q.; Hou, Y.; Qin, Z.; Nguyen, H.T.; Wen, J.; Wei, M.; Yeddu, V.; Saidaminov, M.I.; et al. All-perovskite tandem solar cells with 24.2% certified efficiency and area over 1 cm<sup>2</sup> using surface-anchoring zwitterionic antioxidant. *Nat. Energy* **2020**, *5*, 870–880. [[CrossRef](#)]
146. Lin, R.; Xu, J.; Wei, M.; Wang, Y.; Qin, Z.; Liu, Z.; Wu, J.; Xiao, K.; Chen, B.; Park, S.M.; et al. All-perovskite tandem solar cells with improved grain surface passivation. *Nature* **2022**, *603*, 73–78. [[CrossRef](#)]
147. Wang, M.; Wang, W.; Ma, B.; Shen, W.; Liu, L.; Cao, K.; Chen, S.; Huang, W. Lead-Free Perovskite Materials for Solar Cells. *Nano-Micro Lett.* **2021**, *13*, 62. [[CrossRef](#)]
148. Wang, H.; Wang, Y.; Xuan, Z.; Chen, T.; Zhang, J.; Hao, X.; Wu, L.; Constantinou, I.; Zhao, D. Progress in perovskite solar cells towards commercialization—A review. *Materials* **2021**, *14*, 6569. [[CrossRef](#)]
149. Yang, F.; Jang, D.; Dong, L.; Qiu, S.; Distler, A.; Li, N.; Brabec, C.J.; Egelhaaf, H.-J. Upscaling Solution-Processed Perovskite Photovoltaics. *Adv. Energy Mater.* **2021**, *11*, 2101973. [[CrossRef](#)]
150. Snaith, H.J. Present status and future prospects of perovskite photovoltaics. *Nat. Mater.* **2018**, *17*, 372–376. [[CrossRef](#)]
151. Fu, L.; Li, B.; Li, S.; Yin, L. Future Challenges of the Perovskite Materials. In *Revolution of Perovskite*; Arul, N., Nithya, V., Eds.; Materials Horizons: From Nature to Nanomaterials; Springer: Singapore, 2020; pp. 315–320.
152. Milić, J.V.; Zakeeruddin, S.M.; Grätzel, M. Layered Hybrid Formamidinium Lead Iodide Perovskites: Challenges and Opportunities. *Acc. Chem. Res.* **2021**, *54*, 2729–2740. [[CrossRef](#)]
153. Xiang, W.; Liu, S.F.; Tress, W. A review on the stability of inorganic metal halide perovskites: Challenges and opportunities for stable solar cells. *Energy Environ. Sci.* **2021**, *14*, 2090–2113. [[CrossRef](#)]
154. Cheng, Y.; Peng, Y.; Jen, A.K.-Y.; Yip, H.-L. Development and challenges of metal halide perovskite solar modules. *Sol. RRL* **2022**, *6*, 2100545. [[CrossRef](#)]
155. Liu, Y.; Akin, S.; Hinderhofer, A.; Eickemeyer, F.T.; Zh, H.; Seo, J.-Y.; Zhang, J.; Schreiber, F.; Zhang, H.; Zakeeruddin, S.M.; et al. Stabilization of highly efficient and stable phase-pure FAPbI<sub>3</sub> perovskite solar cells by molecularly tailored 2D-overlayers. *Angew. Chem. Int. Ed.* **2020**, *59*, 15688–15694. [[CrossRef](#)]
156. Schmidt-Mende, L.; Dyakonov, V.; Olthof, S.; Ünlü, F.; Lê, K.M.T.; Mathur, S.; Karabanov, A.D.; Lupascu, D.C.; Herz, L.M.; Hinderhofer, A.; et al. Roadmap on organic–inorganic hybrid perovskite semiconductors and devices. *APL Mater.* **2021**, *9*, 109202. [[CrossRef](#)]
157. Wang, G.; Liao, L.; Chen, L.; Xu, C.; Yao, Y.; Liu, D.; Li, P.; Deng, J.; Song, Q. Perovskite solar cells fabricated under ambient air at room temperature without any post-treatment. *Org. Electron.* **2020**, *86*, 105918. [[CrossRef](#)]
158. Deng, Y.; Van Brackle, C.H.; Dai, X.; Zhao, J.; Chen, B.; Huang, J. Tailoring solvent coordination for high-speed, room-temperature blading of perovskite photovoltaic films. *Sci. Adv.* **2019**, *5*, eaax7537. [[CrossRef](#)]
159. Huckaba, A.J.; Lee, Y.; Xia, R.; Paek, S.; Bassetto, V.C.; Oveisi, E.; Lesch, A.; Kinge, S.; Dyson, P.J.; Girault, H.; et al. Inkjet-Printed Mesoporous TiO<sub>2</sub> and Perovskite Layers for High Efficiency Perovskite Solar Cells. *Energy Technol.* **2019**, *7*, 317–324. [[CrossRef](#)]
160. Ma, L.; Yan, Z.; Zhou, X.; Pi, Y.; Du, Y.; Huang, J.; Wang, K.; Wu, K.; Zhuang, C.; Han, X. A polymer controlled nucleation route towards the generalized growth of organic-inorganic perovskite single crystals. *Nat. Commun.* **2021**, *12*, 2023. [[CrossRef](#)]
161. Berhe, T.A.; Su, W.-N.; Chen, C.-H.; Pan, C.-J.; Cheng, J.-H.; Chen, H.-M.; Tsai, M.-C.; Chen, L.-Y.; Dubale, A.R.; Hwang, B.-J. Organometal halide perovskite solar cells: Degradation and stability. *Energy Environ. Sci.* **2016**, *9*, 323–356. [[CrossRef](#)]
162. Niu, G.; Guo, X.; Wang, L. Review of recent progress in chemical stability of perovskite solar cells. *J. Mater. Chem. A* **2015**, *3*, 8970–8980. [[CrossRef](#)]
163. Wang, Z.; Lin, Q.; Chmiel, F.P.; Sakai, N.; Herz, L.M.; Snaith, H.J. Efficient ambient-air-stable solar cells with 2D–3D heterostructured butylammonium-caesium-formamidinium lead halide perovskites. *Nat. Energy* **2017**, *2*, 17135. [[CrossRef](#)]
164. Leijtens, T.; Eperon, G.E.; Pathak, S.; Abate, A.; Lee, M.M.; Snaith, H.J. Overcoming ultraviolet light instability of sensitized TiO<sub>2</sub> with meso-superstructured organometal tri-halide perovskite solar cells. *Nat. Commun.* **2013**, *4*, 2885. [[CrossRef](#)]

165. Domanski, K.; Correa-Baena, J.-P.; Mine, N.; Nazeeruddin, M.K.; Abate, A.; Saliba, M.; Tress, W.; Hagfeldt, A.; Grätzel, M. Not all that glitters is gold: Metal-migration-induced degradation in perovskite solar cells. *ACS Nano* **2016**, *10*, 6306–6314. [[CrossRef](#)] [[PubMed](#)]
166. Zhang, H.; Wang, H.; Williams, S.T.; Xiong, D.; Zhang, W.; Chueh, C.-C.; Chen, W.; Jen, A.K.-Y. SrCl<sub>2</sub> Derived Perovskite Facilitating a High Efficiency of 16% in Hole-Conductor-Free Fully Printable Mesoscopic Perovskite Solar Cells. *Adv. Mater.* **2017**, *29*, 1606608. [[CrossRef](#)]
167. Liu, D.; Shao, Z.; Li, C.; Pang, S.; Yan, Y.; Cui, G. Structural Properties and Stability of Inorganic CsPbI<sub>3</sub> Perovskites. *Small Struct.* **2021**, *2*, 2000089. [[CrossRef](#)]
168. Li, X.; Tschumi, M.; Han, H.; Babkair, S.S.; Alzubaydi, R.A.; Ansari, A.A.; Habib, S.S.; Nazeeruddin, M.K.; Zakeeruddin, S.M.; Grätzel, M. Outdoor performance and stability under elevated temperatures and long-term light soaking of triple-layer mesoporous perovskite photovoltaics. *Energy Technol.* **2015**, *3*, 551–555. [[CrossRef](#)]
169. Ling, X.; Gao, F.; Cao, Y.; Li, D.; Liu, Q.; Liu, H.; Li, S. Progress on the stability and encapsulation techniques of perovskite solar cells. *Org. Electron.* **2022**, *106*, 106515.
170. Ahmad, J.; Bazaka, K.; Anderson, L.J.; White, R.D.; Jacob, M.V. Materials and methods for encapsulation of OPV: A review. *Renew. Sustain. Energy Rev.* **2013**, *27*, 104–117. [[CrossRef](#)]
171. Wang, Y.; Ahmad, I.; Leung, T.; Lin, J.; Chen, W.; Liu, F.; Ching Ng, A.M.; Zhang, Y.; Djurišić, A.B. Encapsulation and Stability Testing of Perovskite Solar Cells for Real Life Applications. *ACS Mater.* **2022**, *2*, 215–236. [[CrossRef](#)]
172. Rong, Y.; Hou, X.; Hu, Y.; Mei, A.; Liu, L.; Wang, P.; Han, H. Synergy of ammonium chloride and moisture on perovskite crystallization for efficient printable mesoscopic solar cells. *Nat. Commun.* **2017**, *8*, 14555. [[CrossRef](#)]
173. Matteocci, F.; Cinà, L.; Lamanna, E.; Cacovich, S.; Divitini, G.; Midgley, P.A.; Ducati, C.; Di Carlo, A. Encapsulation for long-term stability enhancement of perovskite solar cells. *Nano Energy* **2016**, *30*, 162–172. [[CrossRef](#)]
174. Chen, X.; Cao, H.; Yu, H.; Zhu, H.; Zhou, H.; Yang, L.; Yin, S. Large-area, high-quality organic–inorganic hybrid perovskite thin films via a controlled vapor–solid reaction. *J. Mater. Chem. A* **2016**, *4*, 9124–9132. [[CrossRef](#)]
175. Zhou, H.; Shi, Y.; Dong, Q.; Zhang, H.; Xing, Y.; Wang, K.; Du, Y.; Ma, T. Hole-conductor-free, metal-electrode-free TiO<sub>2</sub>/CH<sub>3</sub>NH<sub>3</sub>PbI<sub>3</sub> heterojunction solar cells based on a low-temperature carbon electrode. *J. Phys. Chem. Lett.* **2014**, *5*, 3241–3246. [[CrossRef](#)] [[PubMed](#)]
176. Kwon, Y.-S.; Lim, J.; Yun, H.-J.; Kim, Y.-H.; Park, T. A diketopyrrolopyrrole-containing hole transporting conjugated polymer for use in efficient stable organic–inorganic hybrid solar cells based on a perovskite. *Energy Environ. Sci.* **2014**, *7*, 1454–1460. [[CrossRef](#)]
177. Chang, C.-Y.; Lee, K.-T.; Huang, W.-K.; Siao, H.-Y.; Chang, Y.-C. High-performance, air-stable, low-temperature processed semitransparent perovskite solar cells enabled by atomic layer deposition. *Chem. Mater.* **2015**, *27*, 5122–5130. [[CrossRef](#)]
178. Hashmi, S.G.; Tiihonen, A.; Martineau, D.; Ozkan, M.; Vivo, P.; Kaunisto, K.; Ulla, V.; Zakeeruddin, S.M.; Grätzel, M. Long term stability of air processed inkjet infiltrated carbon-based printed perovskite solar cells under intense ultra-violet light soaking. *J. Mater. Chem. A* **2017**, *5*, 4797–4802. [[CrossRef](#)]
179. Eperon, G.E.; Stranks, S.D.; Menelaou, C.; Johnston, M.B.; Herz, L.M.; Snaith, H.J. Formamidinium lead trihalide: A broadly tunable perovskite for efficient planar heterojunction solar cells. *Energy Environ. Sci.* **2014**, *7*, 982–988. [[CrossRef](#)]
180. Filip, M.R.; Eperon, G.E.; Snaith, H.J.; Giustino, F. Steric engineering of metal-halide perovskites with tunable optical band gaps. *Nat. Commun.* **2014**, *5*, 5757. [[CrossRef](#)]
181. Ren, M.; Qian, X.; Chen, Y.; Wang, T.; Zhao, Y. Potential lead toxicity and leakage issues on lead halide perovskite photovoltaics. *J. Hazard. Mater.* **2022**, *426*, 127848. [[CrossRef](#)]
182. Flora, G.; Gupta, D.; Tiwari, A. Toxicity of lead: A review with recent updates. *Interdiscip. Toxicol.* **2012**, *5*, 47–58. [[CrossRef](#)]
183. Chen, C.-H.; Cheng, S.-N.; Cheng, L.; Wang, Z.-K.; Liao, L.-S. Toxicity, Leakage, and Recycling of Lead in Perovskite Photovoltaics. *Adv. Energy Mater.* **2023**, *13*, 2204144. [[CrossRef](#)]
184. Kim, G.-Y.; Kim, K.; Kim, H.-J.; Jung, H.-S.; Jeon, I.; Lee, J.W. Sustainable and environmentally viable perovskite solar cells. *EcoMat* **2023**, *5*, e12319. [[CrossRef](#)]
185. Wu, C.; Zhang, Q.; Liu, Y.; Luo, W.; Guo, X.; Huang, Z.; Ting, H.; Sun, W.; Zhong, X.; Wei, S.; et al. The dawn of lead-free perovskite solar cell: Highly stable double perovskite Cs<sub>2</sub>AgBiBr<sub>6</sub> film. *Adv. Sci.* **2018**, *5*, 1700759. [[CrossRef](#)] [[PubMed](#)]
186. Hartono, N.T.P.; Thapa, J.; Tiihonen, A.; Oviedo, F.; Batali, C.; Yoo, J.J.; Liu, Z.; Li, R.; Marrón, D.F.; Bawendi, M.G.; et al. How machine learning can help select capping layers to suppress perovskite degradation. *Nat. Commun.* **2020**, *11*, 4172. [[CrossRef](#)]
187. Herz, L.M. How lattice dynamics moderate the electronic properties of metal-halide perovskites. *J. Phys. Chem. Lett.* **2018**, *9*, 6853–6863. [[CrossRef](#)] [[PubMed](#)]
188. Gu, E.; Tang, X.; Langner, S.; Duchstein, P.; Zhao, Y.; Levchuk, I.; Kalancha, V.; Stubhan, T.; Hauch, J.; Egelhaaf, H.J.; et al. Robot-based high-throughput screening of antisolvents for lead halide perovskites. *Joule* **2020**, *4*, 1806–1822. [[CrossRef](#)]
189. Byrne, F.P.; Jin, S.; Paggiola, G.; Petchey, T.H.M.; Clark, J.H.; Farmer, T.J.; Hunt, A.J.; McElroy, C.R.; Sherwood, J. Tools and techniques for solvent selection: Green solvent selection guides. *Sustain. Chem. Process.* **2016**, *4*, 7. [[CrossRef](#)]
190. Chen, J.; Park, N.-G. Causes and Solutions of Recombination in Perovskite Solar Cells. *Adv. Mater.* **2019**, *31*, 1803019. [[CrossRef](#)]
191. Kiermasch, D.; Fischer, M.; Gil-Escrig, L.; Baumann, A.; Bolink, H.J.; Dyakonov, V.; Tvingstedt, K. Reduced Recombination Losses in Evaporated Perovskite Solar Cells by Postfabrication Treatment. *Sol. RRL* **2021**, *5*, 2100400. [[CrossRef](#)]

192. Zhang, H.; Ji, X.; Yao, H.; Fan, Q.; Yu, B.; Li, J. Review of the efficiency improvement effort of perovskite solar cells. *Sol. Energy* **2022**, *233*, 421–434. [[CrossRef](#)]
193. Cheng, H.; Li, Y.; Zhong, Y. Towards cost-efficient and stable perovskite solar cells and modules: Utilization of self-assembled monolayers. *Mater. Chem. Front.* **2023**. [[CrossRef](#)]
194. Wang, S.; Peng, Y.; Li, L.; Zhou, Z.; Liu, Z.; Zhou, S.; Yao, M. Impact of loss mechanisms on performances of perovskite solar cells. *Phys. B Condens. Matter* **2022**, *647*, 414363. [[CrossRef](#)]
195. Du, B.; He, K.; Zhao, X.; Li, B. Defect Passivation Scheme toward High-Performance Halide Perovskite Solar Cells. *Polymers* **2023**, *15*, 2010. [[CrossRef](#)]
196. Lee, S.-W.; Bae, S.-H.; Kim, D.-H.; Lee, H.-S. Historical Analysis of High-Efficiency, Large-Area Solar Cells: Toward Upscaling of Perovskite Solar Cells. *Adv. Mater.* **2020**, *32*, 2002202. [[CrossRef](#)]
197. Zhao, J.; Zheng, X.; Deng, Y.; Li, T.; Shao, Y.; Gruverman, A.; Shield, J.; Huang, J. Is Cu a stable electrode material in hybrid perovskite solar cells for a 30-year lifetime? *Energy Environ. Sci.* **2016**, *9*, 3650–3656. [[CrossRef](#)]
198. Binek, A.; Petrus, M.L.; Huber, N.; Bristow, H.; Hu, Y.; Bein, T.; Docampo, P. Recycling perovskite solar cells to avoid lead waste. *ACS Appl. Mater. Interfaces* **2016**, *8*, 12881–12886. [[CrossRef](#)]
199. Liu, F.-W.; Biesold, G.; Zhang, M.; Lawless, R.; Correa-Baena, J.-P.; Chueh, Y.-L.; Lin, Z. Recycling and recovery of perovskite solar cells. *Materials Today* **2021**, *43*, 185–197. [[CrossRef](#)]
200. Vidal, R.; Alberola-Borràs, J.-A.; Sánchez-Pantoja, N.; Mora-Seró, I. Comparison of Perovskite Solar Cells with other Photovoltaics Technologies from the Point of View of Life Cycle Assessment. *Adv. Energy Sustain. Res.* **2021**, *2*, 2000088. [[CrossRef](#)]
201. Sofia, A.E.; Wang, H.; Bruno, A.; Cruz-Campa, J.L.; Buonassisi, T.; Peters, I.M. Roadmap for cost-effective, commercially-viable perovskite silicon tandems for the current and future PV market. *Sustain. Energy Fuels* **2020**, *4*, 852–862. [[CrossRef](#)]
202. Chang, N.L.; Ho-Baillie, A.W.Y.; Basore, P.A.; Young, T.L.; Evans, R.; Egan, R.J. A manufacturing cost estimation method with uncertainty analysis and its application to perovskite on glass photovoltaic modules. *Prog. Photovolt. Res. Appl.* **2017**, *25*, 390–405. [[CrossRef](#)]
203. Chang, N.L.; Ho-Baillie, A.W.Y.; Vak, D.; Gao, M.; Green, M.A.; Egan, R.J. Manufacturing cost and market potential analysis of demonstrated roll-to-roll perovskite photovoltaic cell processes. *Sol. Energy Mater. Sol. Cells* **2018**, *174*, 314–324. [[CrossRef](#)]
204. Hutchins, M. The Economics of Solar Perovskite Manufacturing. *PV Magazine*. 22 September 2022. Available online: <https://www.pv-magazine.com/2022/09/02/the-economics-of-perovskite-solar-manufacturing/> (accessed on 25 April 2023).
205. Čulík, P.; Brooks, K.; Momblona, C.; Adams, M.; Kinge, S.; Maréchal, F.; Dyson, P.J.; Nazeeruddin, M.K. Design and Cost Analysis of 100 MW Perovskite Solar Panel Manufacturing Process in Different Locations. *ACS Energy Lett.* **2022**, *7*, 3039–3044. [[CrossRef](#)]
206. The SunShot Initiative: Making Solar Energy Affordable for All Americans. U.S. Department of Energy (DOE). Available online: <https://www.energy.gov/eere/solar/sunshot-initiative> (accessed on 10 July 2023).
207. Li, Z.; Zhao, Y.; Wang, X.; Sun, Y.; Zhao, Z.; Li, Y.; Zhou, H.; Chen, Q. Cost Analysis of Perovskite Tandem Photovoltaics. *Joule* **2018**, *2*, 1559–1572. [[CrossRef](#)]
208. Global Industry Analysis, Size, Share, Growth, Trends, Regional Outlook, and Forecast 2023–2032. Available online: <https://www.precedenceresearch.com/perovskite-solar-cell-market> (accessed on 6 July 2023).
209. Global Opportunity Analysis and Industry Forecast, 2021–2030. Fortune Business Insight. Available online: <https://www.fortunebusinessinsights.com/industry-reports/perovskite-solar-cell-market-101556> (accessed on 6 July 2023).

**Disclaimer/Publisher’s Note:** The statements, opinions and data contained in all publications are solely those of the individual author(s) and contributor(s) and not of MDPI and/or the editor(s). MDPI and/or the editor(s) disclaim responsibility for any injury to people or property resulting from any ideas, methods, instructions or products referred to in the content.